Supporting Information

One-pot synthesis of conjugated triphenylamine macrocycles and their complexation with fullerenes

Yingbo Lu,[a] Shinji Kanehashi,[a] Kazushi Minegishi,[a] Shu-Ping Wang,[b] Jin Cheng,[a] Kenji Ogino*[a] and Shijun Li*[b]

[a] Guaduate School of Bio-Applications and Systems Engineering, Tokyo University of Agriculture and Technology, 2-24-16 Nakacho, Tokyo, Japan
[b] College of Material, Chemistry and Chemical Engineering, Hangzhou Normal University, Hangzhou, 311121, P. R. China.

Email address: kogino@cc.tuat.ac.jp; l_shijun@hznu.edu.cn

Table of contents

1. *NMR and MS spectra* S2
2. *Solubility of COTPAs* S13
3. *UV-vis and fluorescence spectra* S14
4. *Determination of binding stoichiometries* S18
5. *Measurement of binding constants (K_a)* S30
6. *Side view of DFT optimized structures* S42

1. NMR and MS spectra

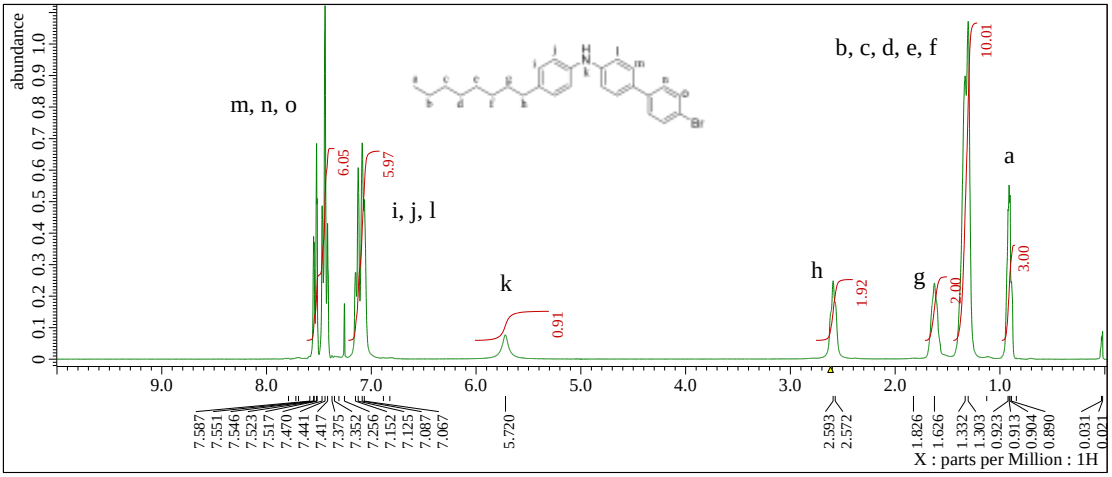

Fig. S1 ^{1}H NMR (300 MHz, $CDCl_3$) spectrum of monomer **1**.

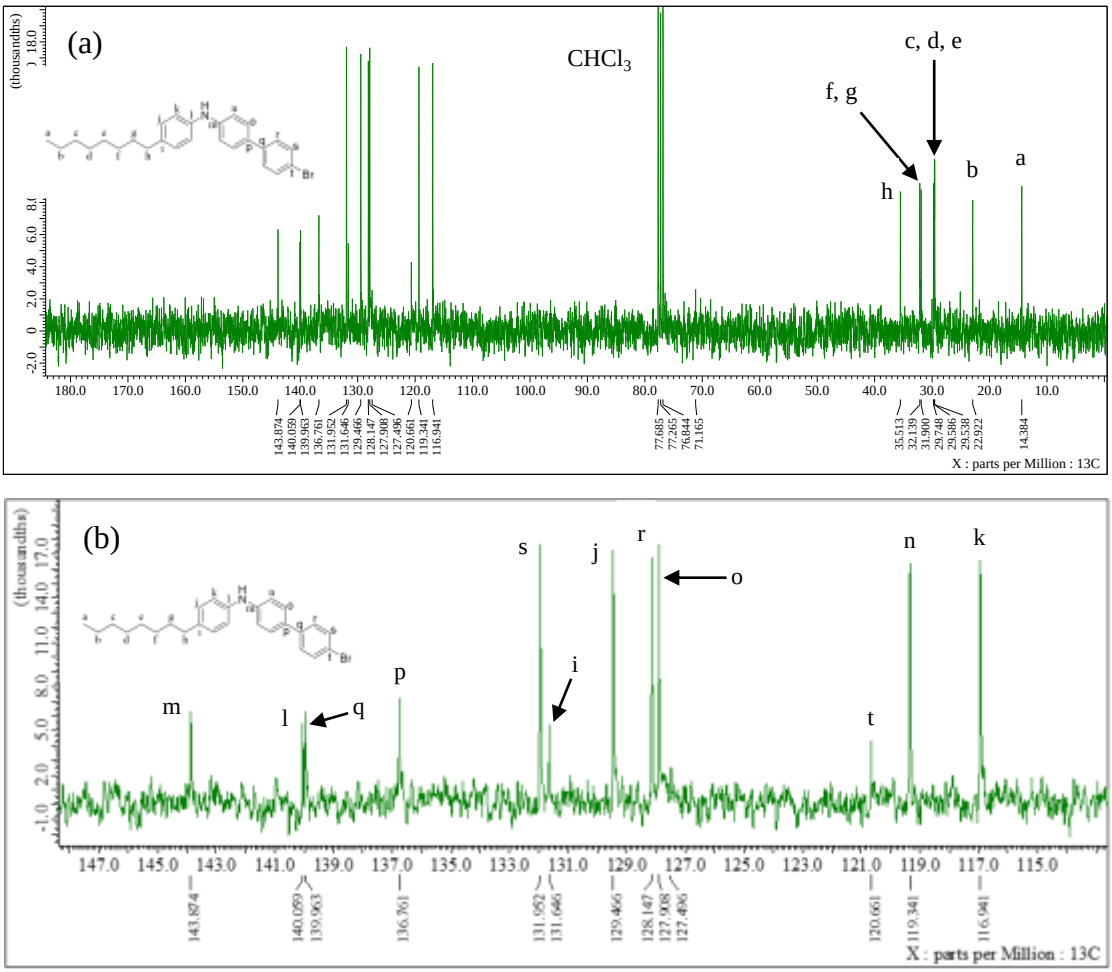

Fig. S2 (a) ^{13}C NMR (75 MHz, $CDCl_3$) spectrum of monomer **1**; and (b) enlarged ^{13}C NMR (75 MHz, $CDCl_3$) spectrum of monomer **1**.

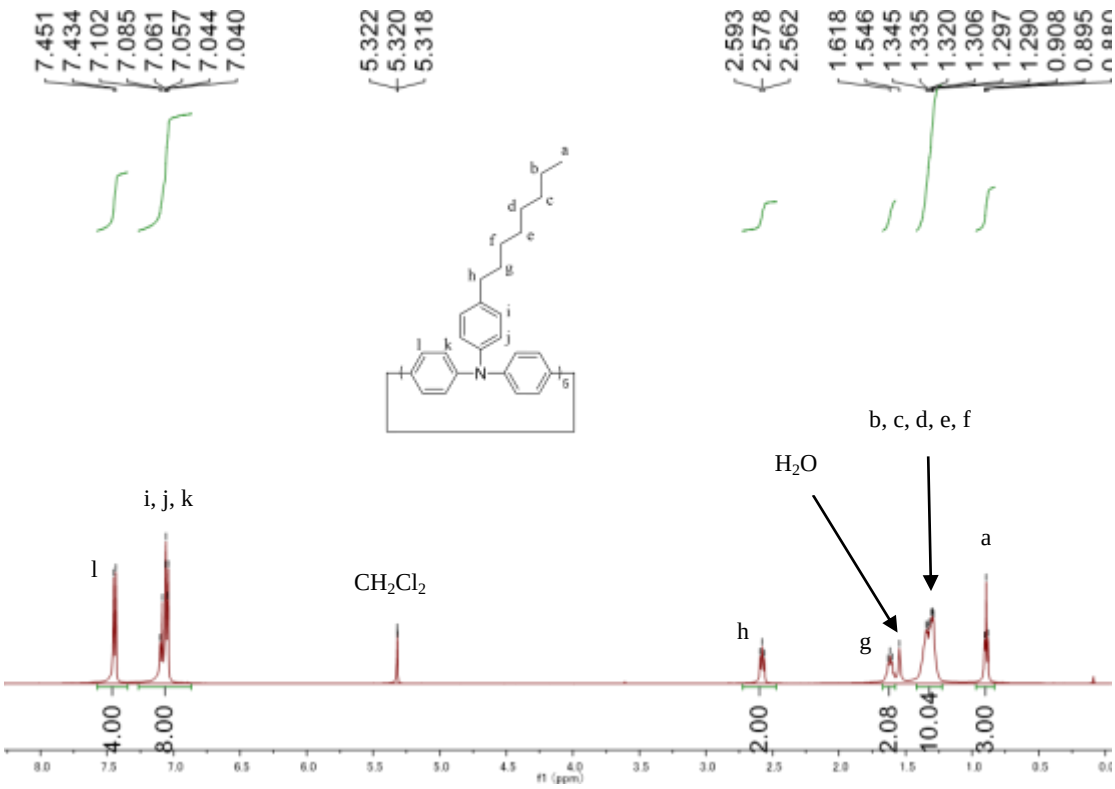

Fig. S3 ^{1}H NMR (500 MHz, CD_2Cl_2) spectrum of **COTPA [5]**.

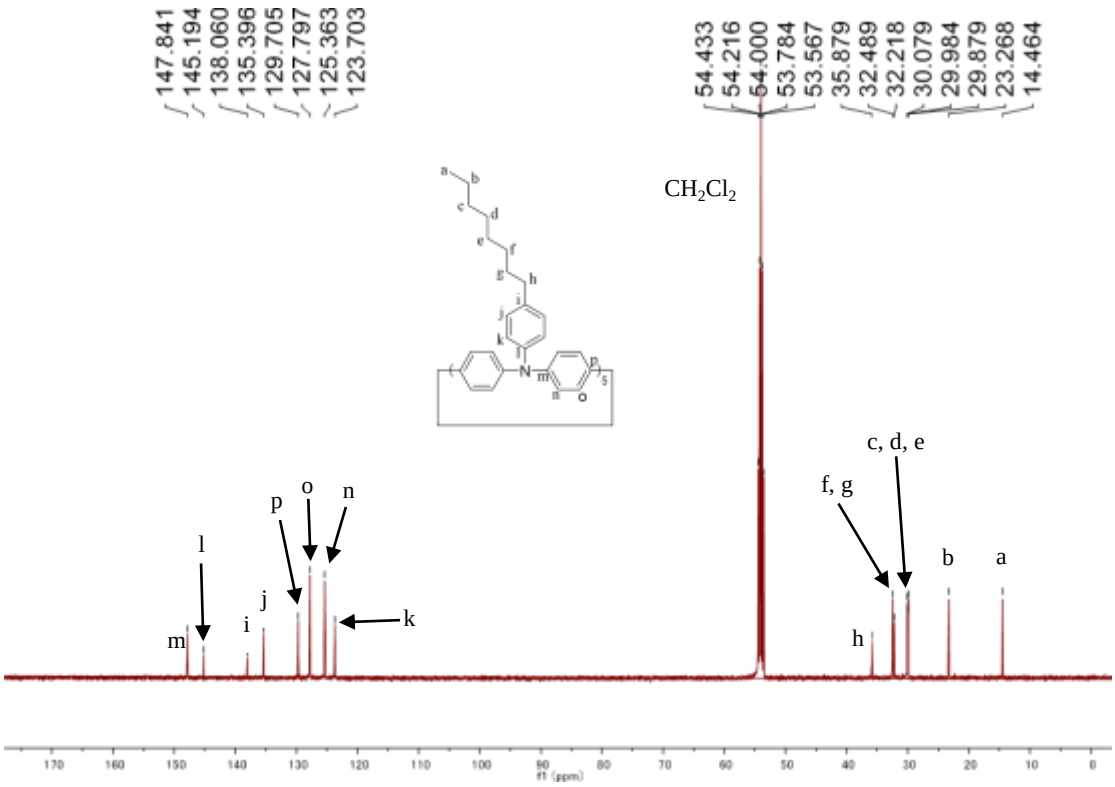

Fig. S4 ^{13}C NMR (126 MHz, CD_2Cl_2) spectrum of **COTPA [5]**.

(a)

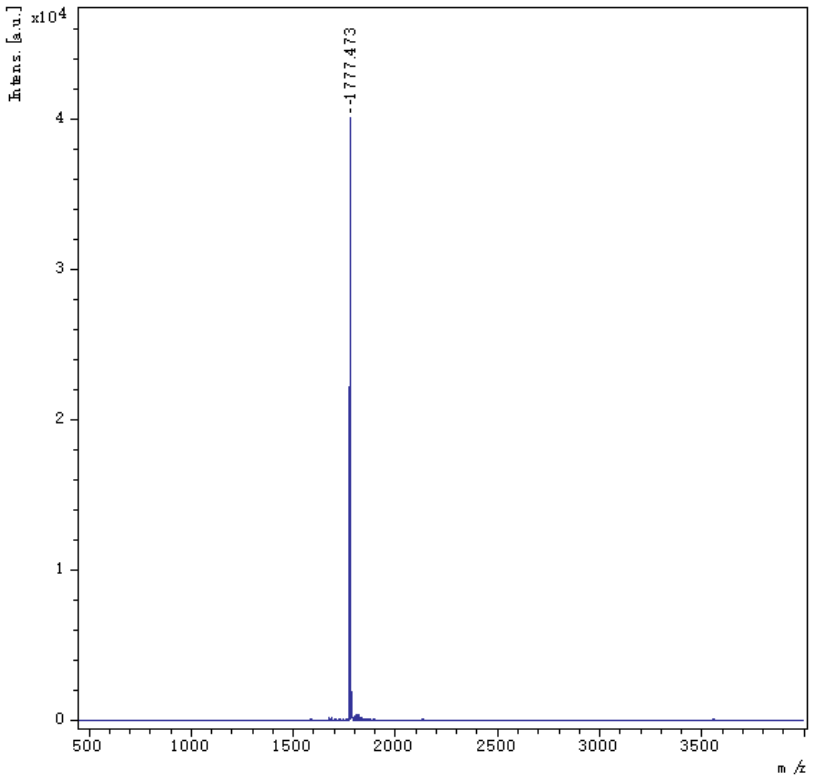

(b)

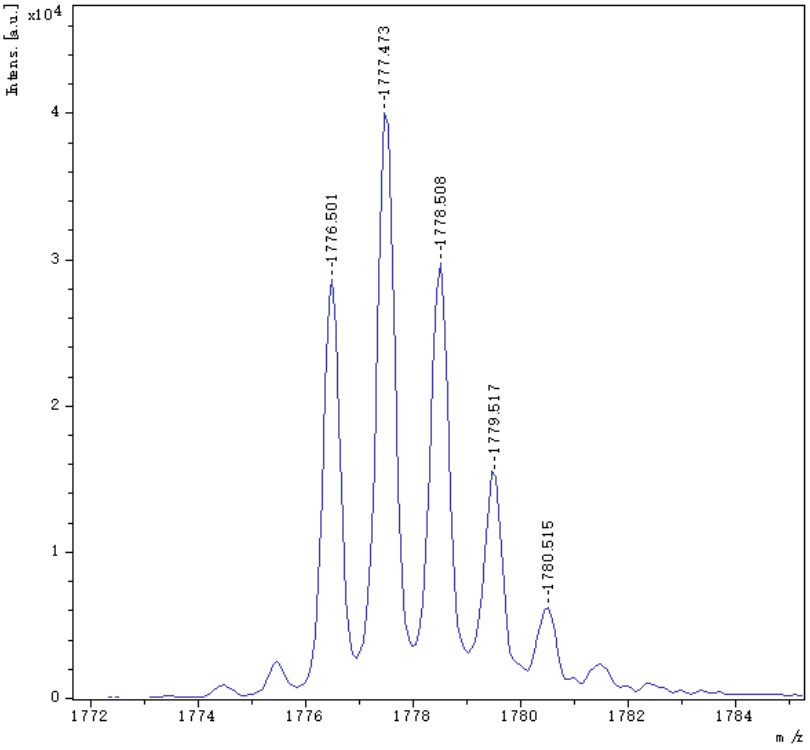

Fig. S5 (a) MALDI-TOF-MS spectrum of **COTPA [5]**, and (b) its enlarged spectrum (matrix: *trans*-2-[3-(4-*tert*-butylphenyl)-2-methyl-2-propenylidene]malononitrile).

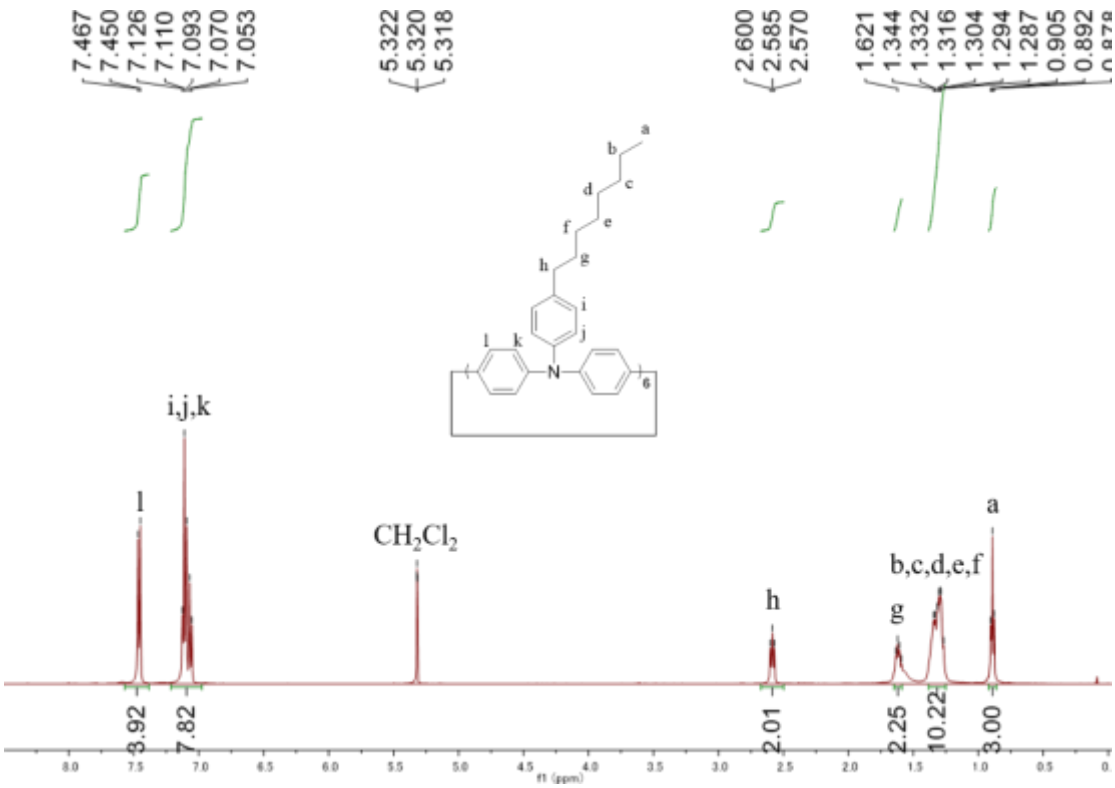

Fig. S6 ^{1}H NMR (500 MHz, CD_2Cl_2) spectrum of **COTPA [6]**.

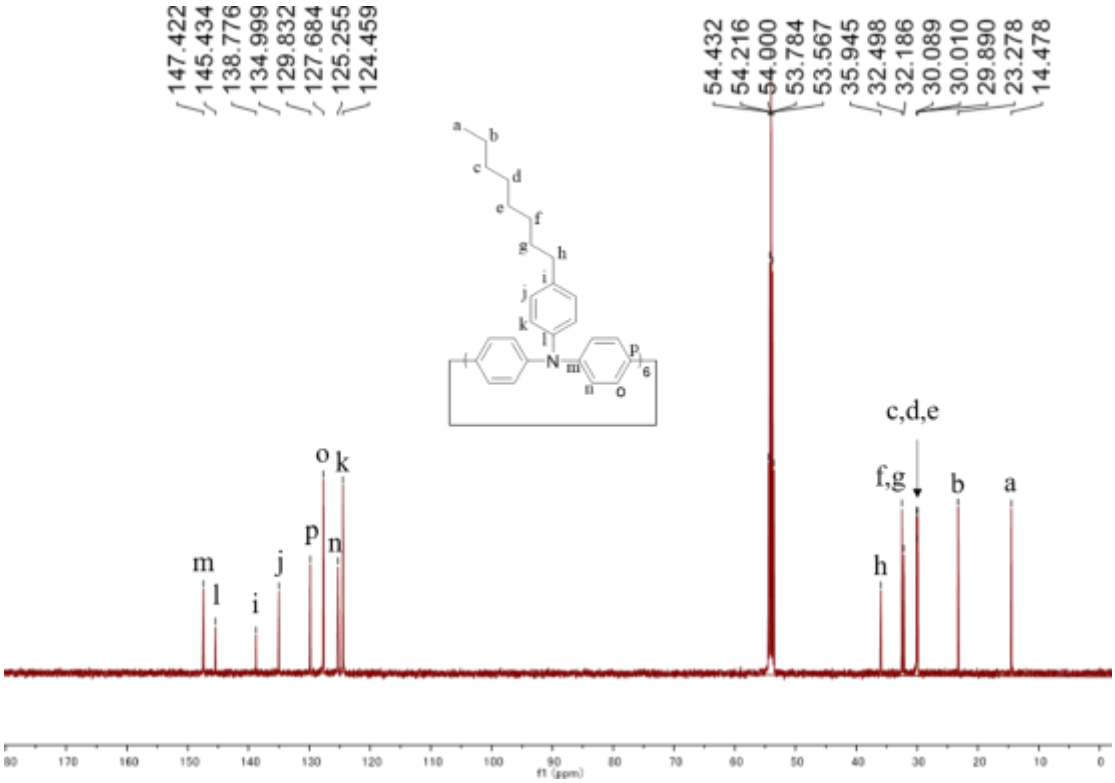

Fig. S7 ^{13}C NMR (126 MHz, CD_2Cl_2) spectrum of **COTPA [6]**.

(a)

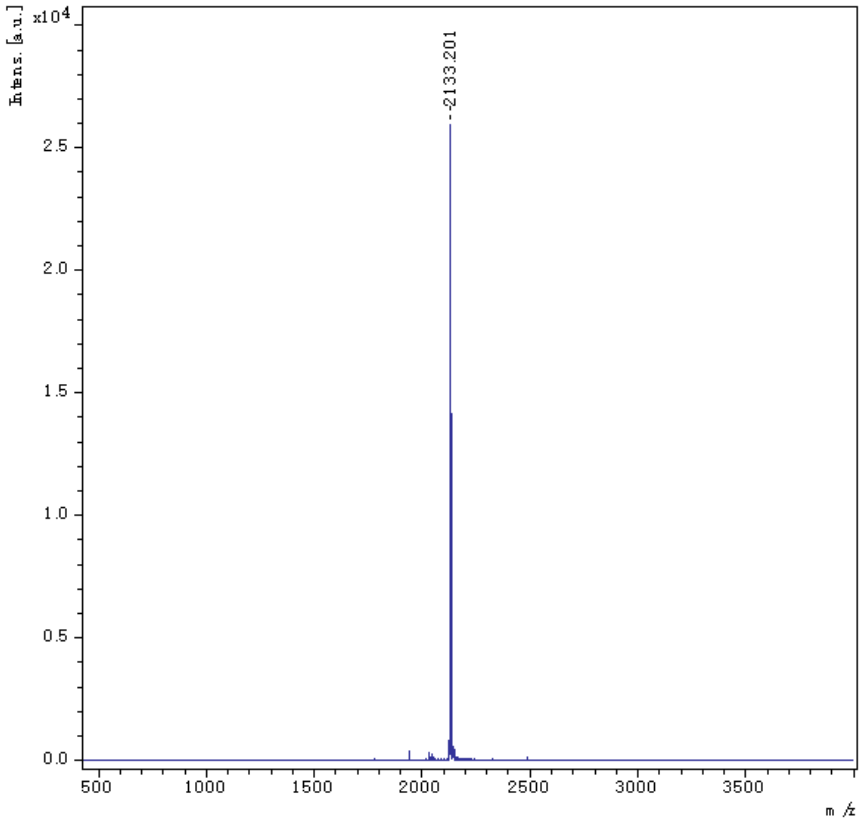

(b)

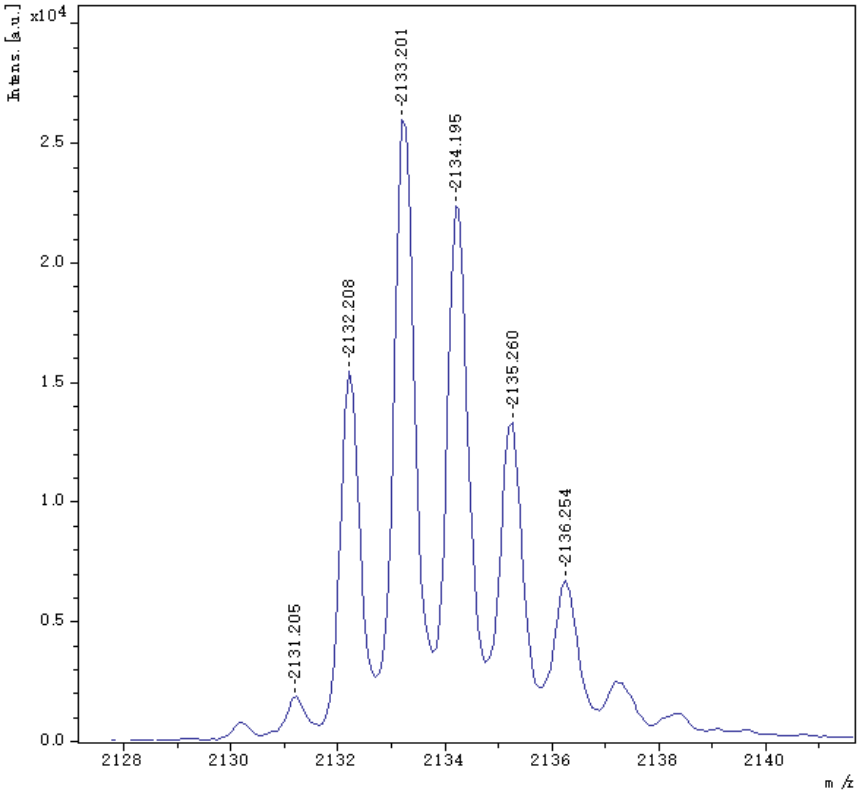

Fig. S8 (a) MALDI-TOF-MS spectrum of **COTPA [6]**, and (b) its enlarged spectrum (matrix: *trans*-2-[3-(4-*tert*-Butylphenyl)-2-methyl-2-propenylidene]malononitrile).

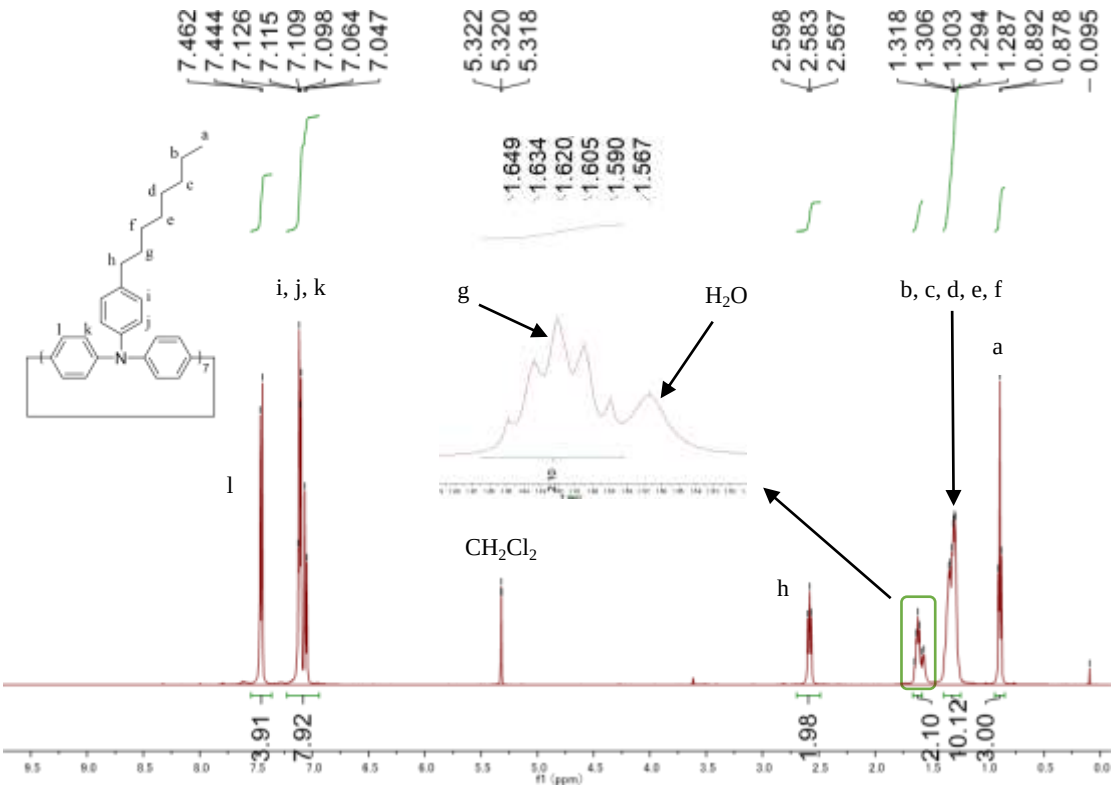

Fig. S9 ^{1}H NMR (500 MHz, CD_2Cl_2) spectrum of **COTPA [7]**.

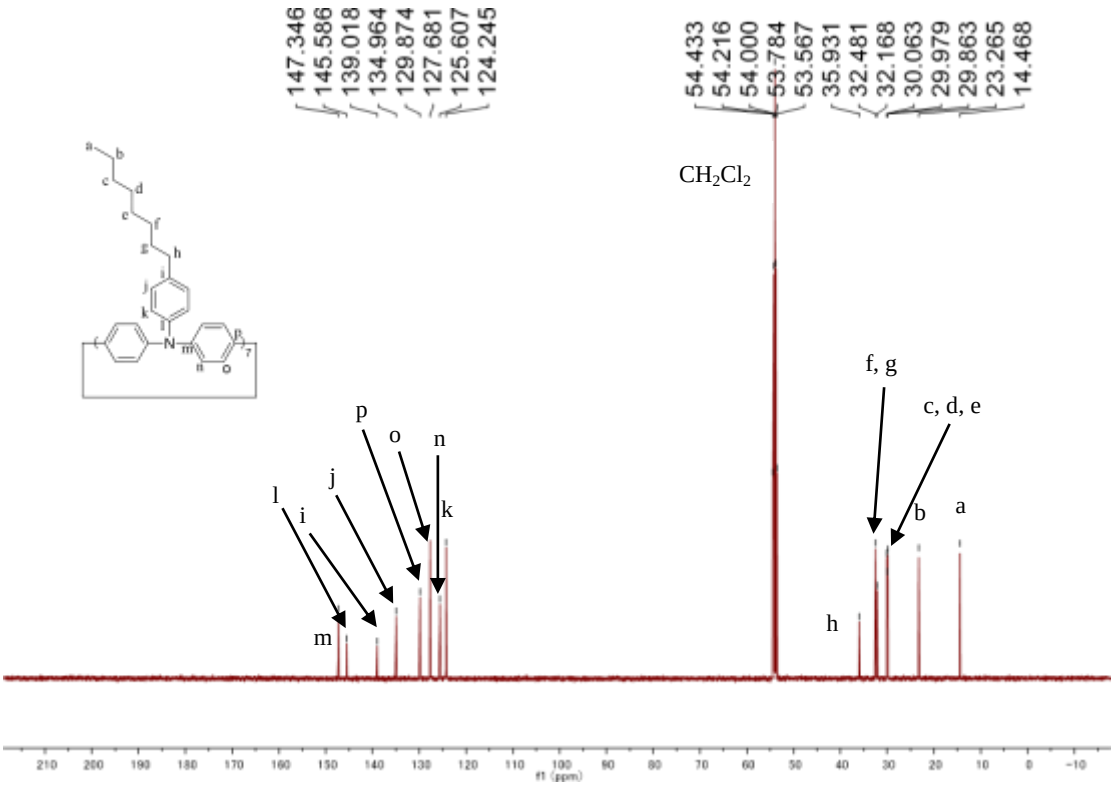

Fig. S10 ^{13}C NMR (126 MHz, CD_2Cl_2) spectrum of **COTPA [7]**.

(a)

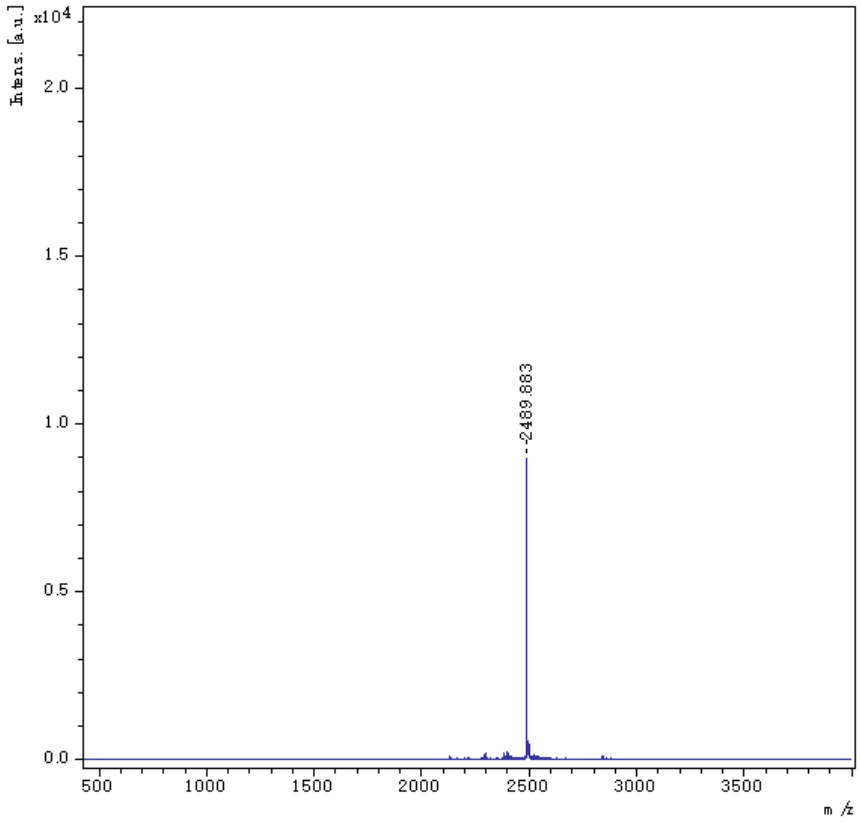

(b)

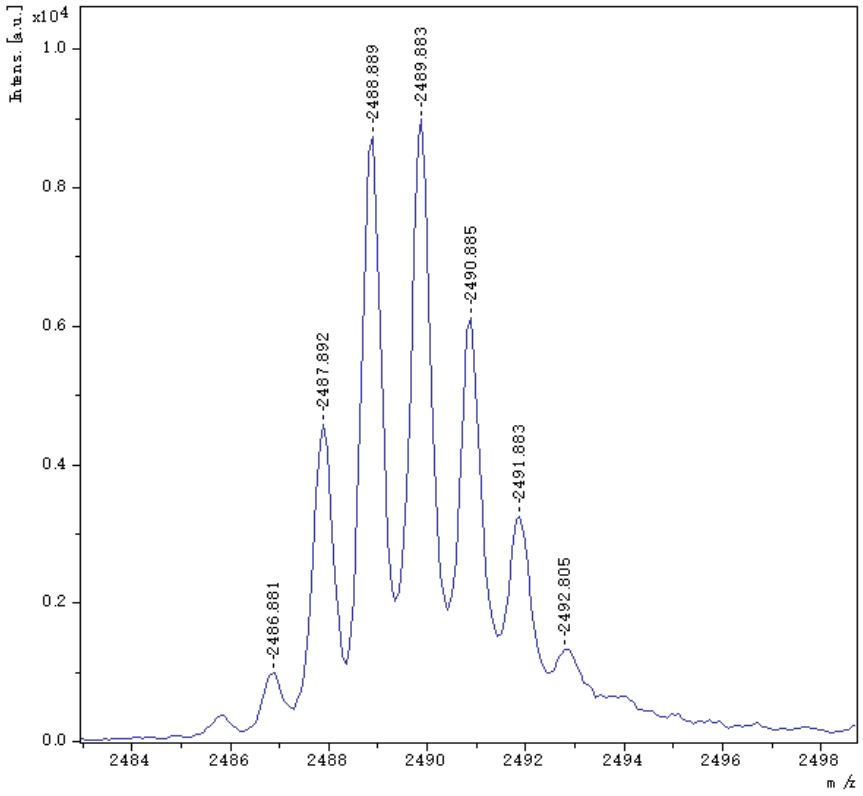

Fig. S11 (a) MALDI-TOF-MS spectrum of **COTPA [7]**, and (b) its enlarged spectrum (matrix: *trans*-2-[3-(4-*tert*-Butylphenyl)-2-methyl-2-propenylidene]malononitrile).

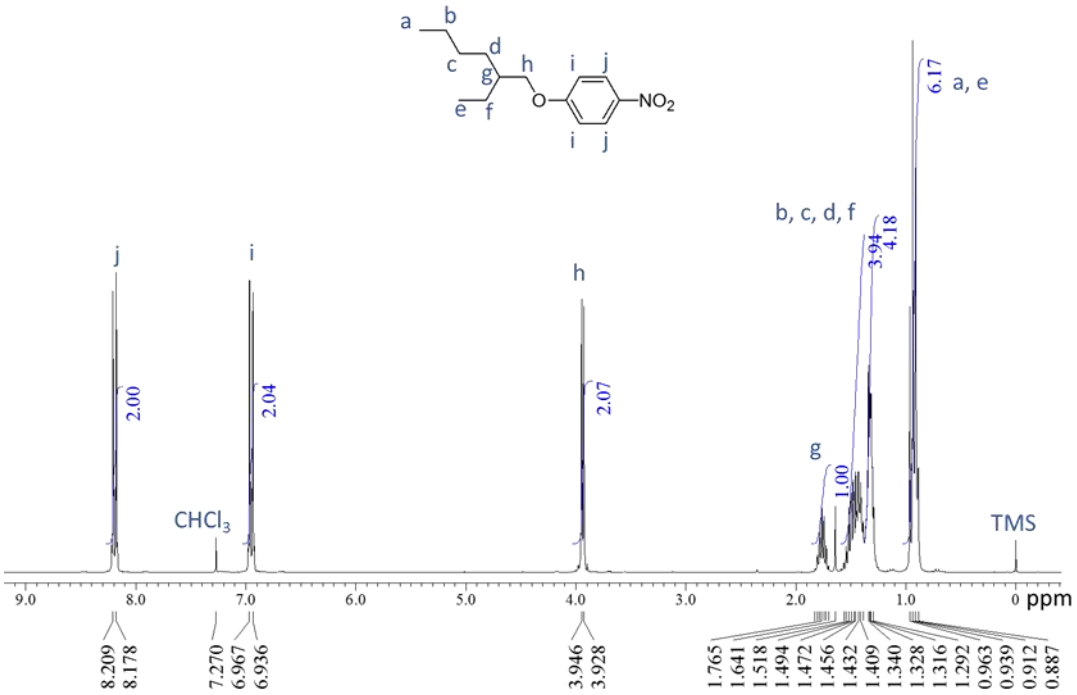

Fig. S12 ^{1}H NMR (300 MHz, $CDCl_3$) spectrum of 4-[(2-ethylhexyl)oxy]nitrobenzene.

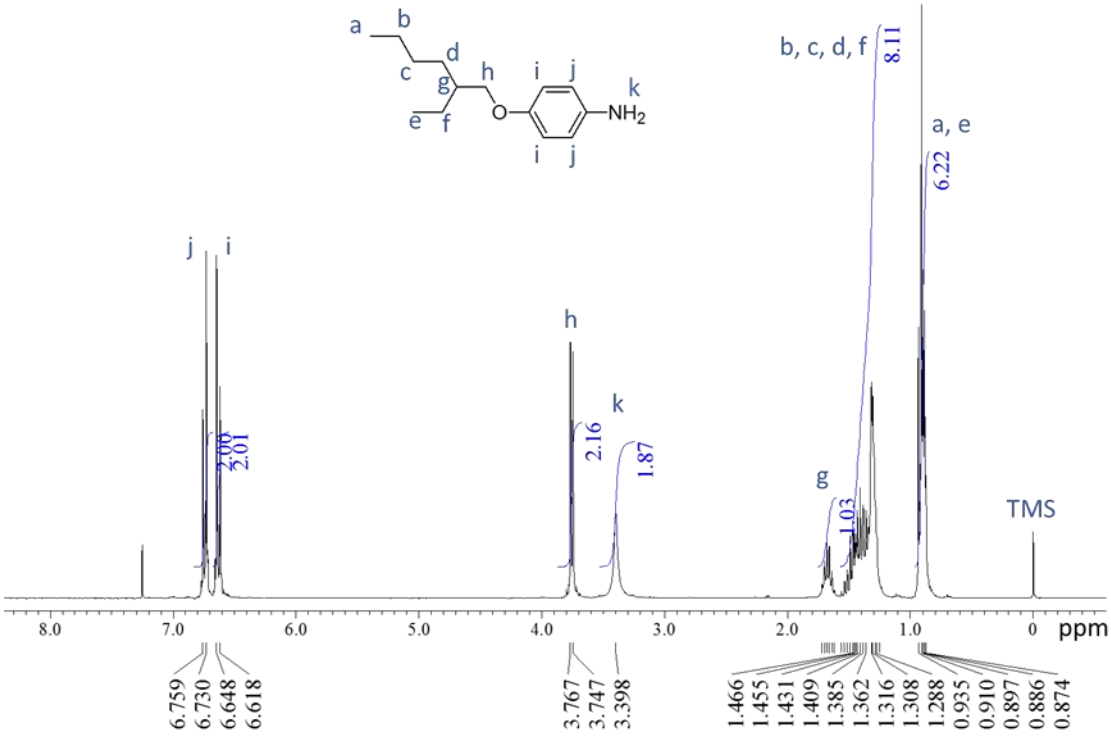

Fig S13. ^{1}H NMR (300 MHz, $CDCl_3$) spectrum of 4-[(2-ethylhexyl)oxy]aniline.

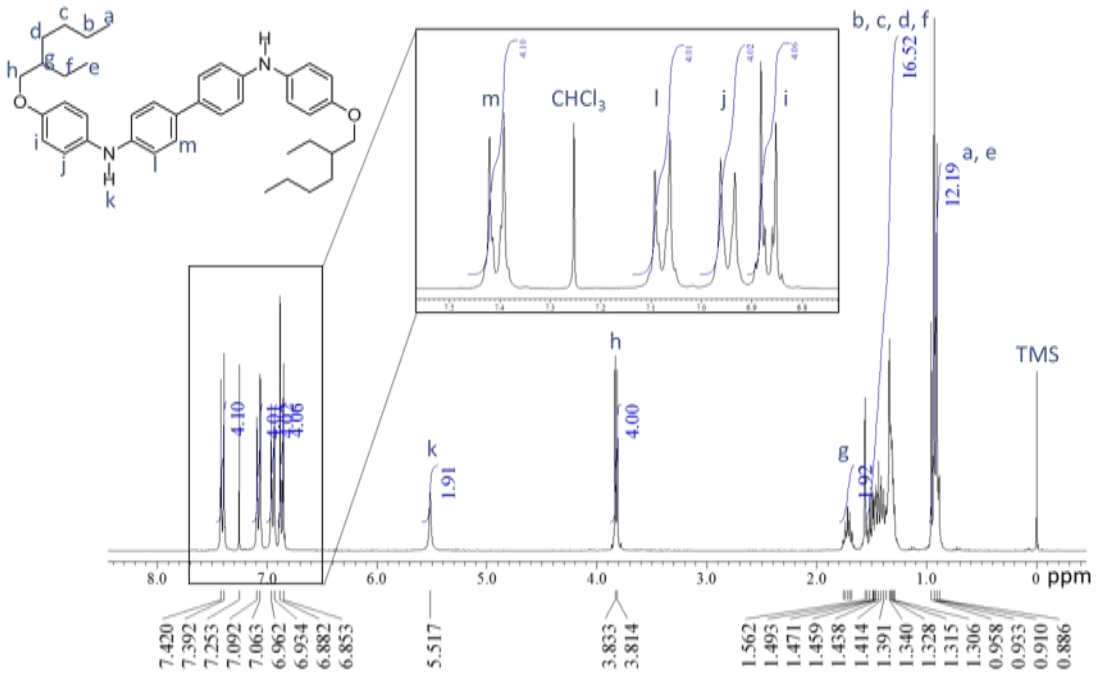

Fig S14. ^{1}H NMR (300 MHz, $CDCl_3$) spectrum of monomer **2**.

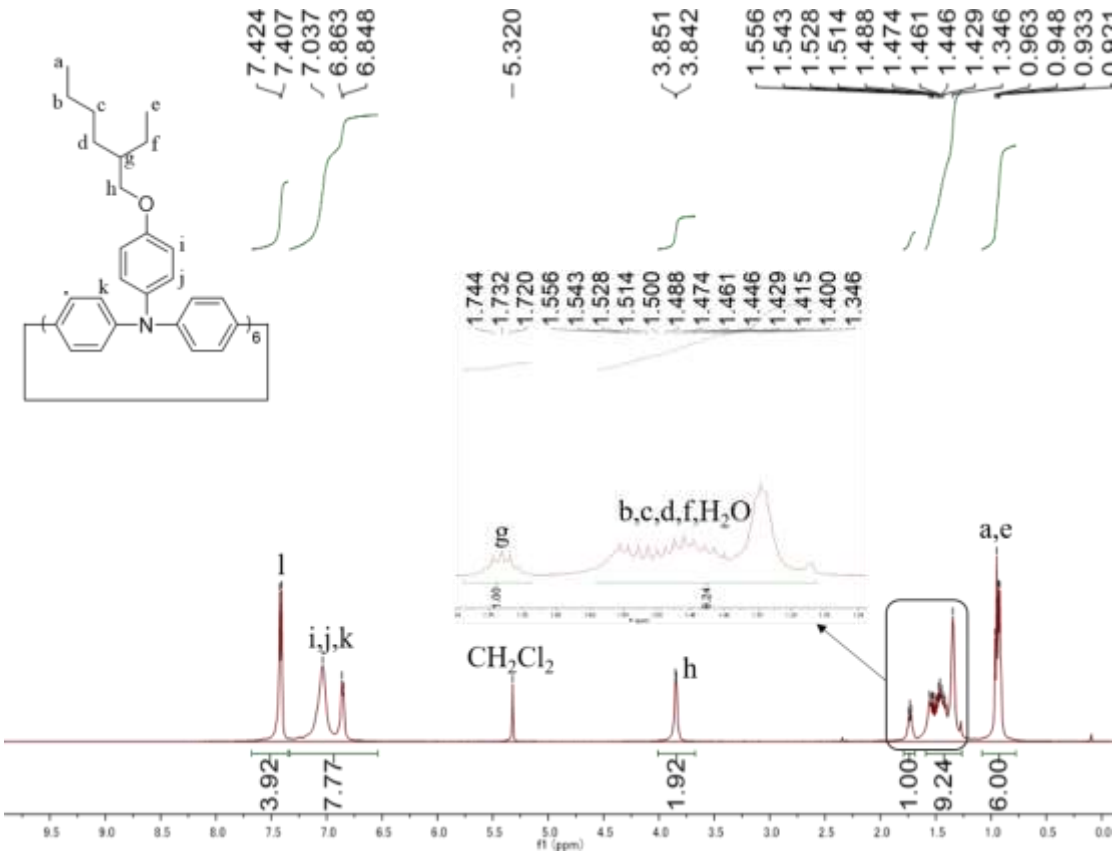

Fig. S15 ^{1}H NMR (500 MHz, CD_2Cl_2) spectrum of **CETPA [6]**.

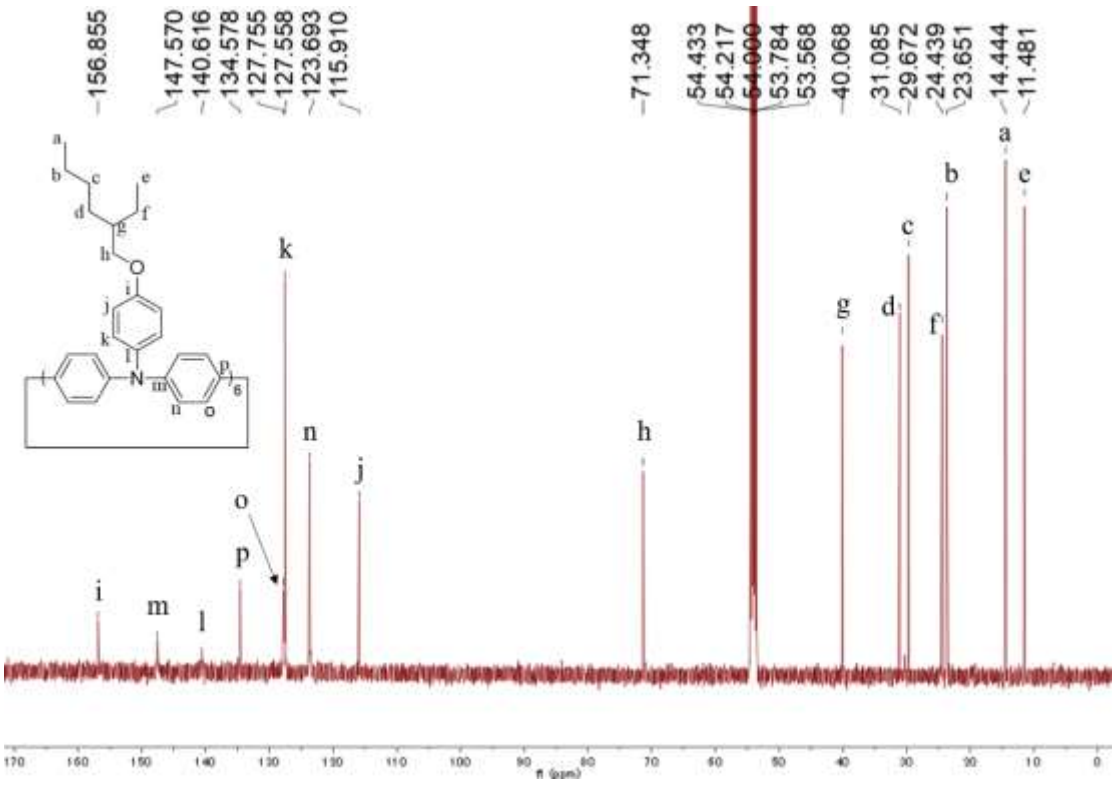

Fig. S16 ^{13}C NMR (126 MHz, CD_2Cl_2) spectrum of **CETPA [6]**.

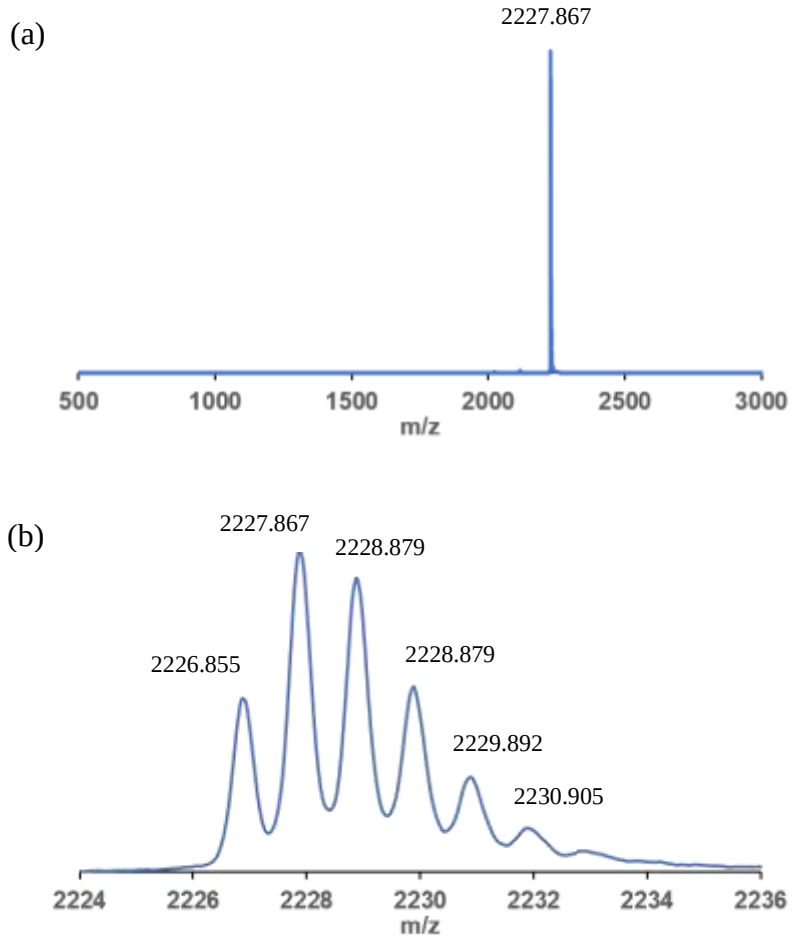

Fig. S17 (a) MALDI-TOF-MS spectrum of **CETPA [6]**, and (b) its enlarged spectrum (matrix: *trans*-2-[3-(4-*tert*-Butylphenyl)-2-methyl-2-propenylidene]malononitrile).

2. Solubility of COTPAs

Table S1. Solubility of COTPAs in toluene, chlorobenzene and chloroform.

	COTPA [5]	COTPA [6]	COTPA [7]
toluene	O	X	O
chlorobenzene	O	Δ	O
chloroform	O	O	O

X: less than 10 mg/mL
Δ: from 10 to 20 mg/mL
O: more than 20 mg/mL

3. UV-vis and fluorescence spectra

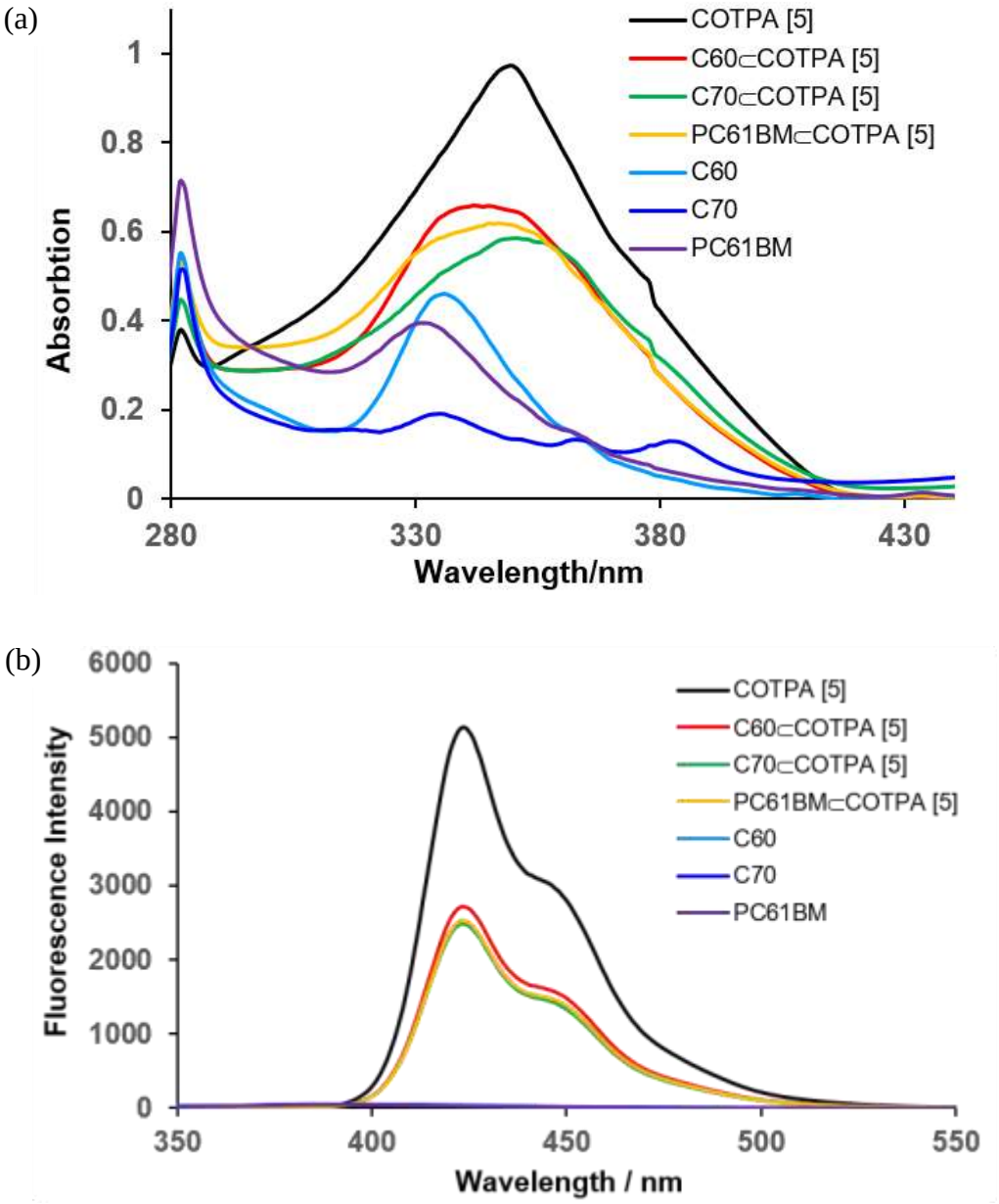

Fig. S18 (a) UV-vis and (b) fluorescence (λ_{ex} = 300 nm in toluene, 5×10^{-6} M, 298 K) spectra of **COTPA [5]**, C_{60}⊂**COTPA [5]**, C_{70}⊂**COTPA [5]**, $PC_{61}BM$⊂**COTPA [5]**, C_{60}, C_{70} and $PC_{61}BM$.

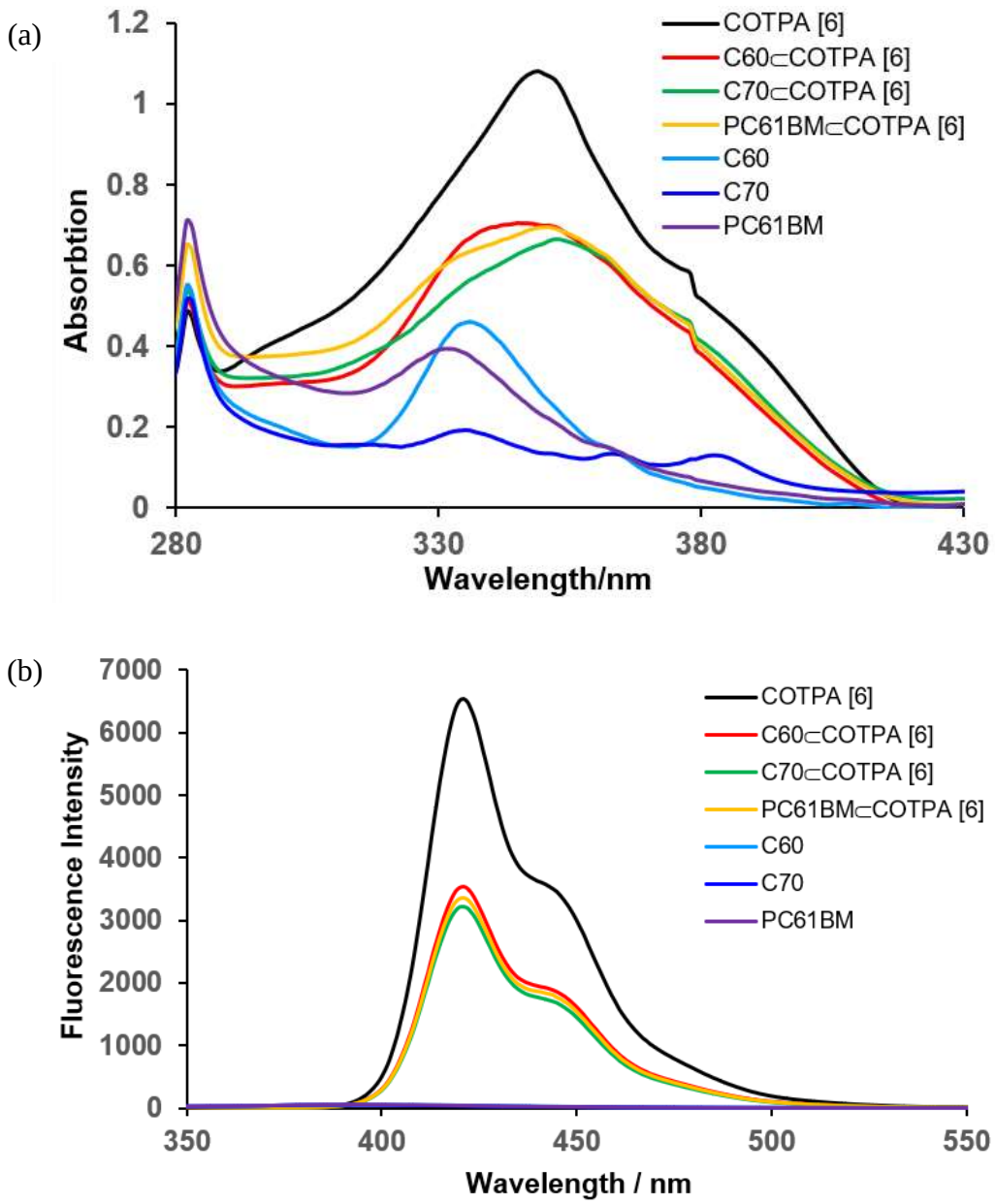

Fig. S19 (a) UV-vis and (b) fluorescence (λ_{ex} = 300 nm in toluene, 5×10^{-6} M, 298 K) spectra of **COTPA [6]**, C_{60}⊂**COTPA [6]**, C_{70}⊂**COTPA [6]**, $PC_{61}BM$⊂**COTPA [6]**, C_{60}, C_{70} and $PC_{61}BM$.

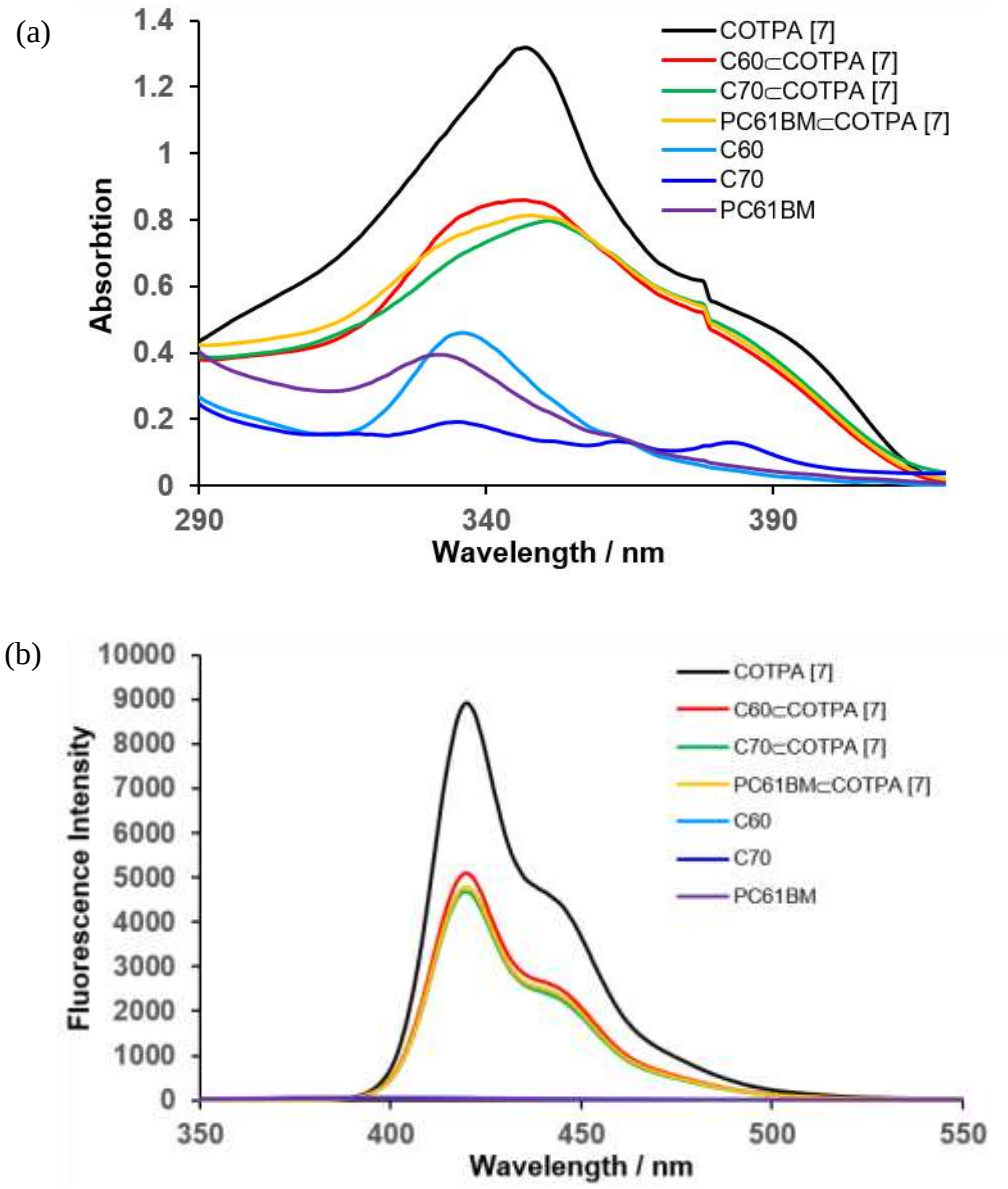

Fig. S20 (a) UV-vis and (b) fluorescence (λ_{ex} = 300 nm in toluene, 5×10^{-6} M, 298 K) spectra of **COTPA [7]**, C_{60}⊂**COTPA [7]**, C_{70}⊂**COTPA [7]**, $PC_{61}BM$⊂**COTPA [7]**, C_{60}, C_{70} and $PC_{61}BM$.

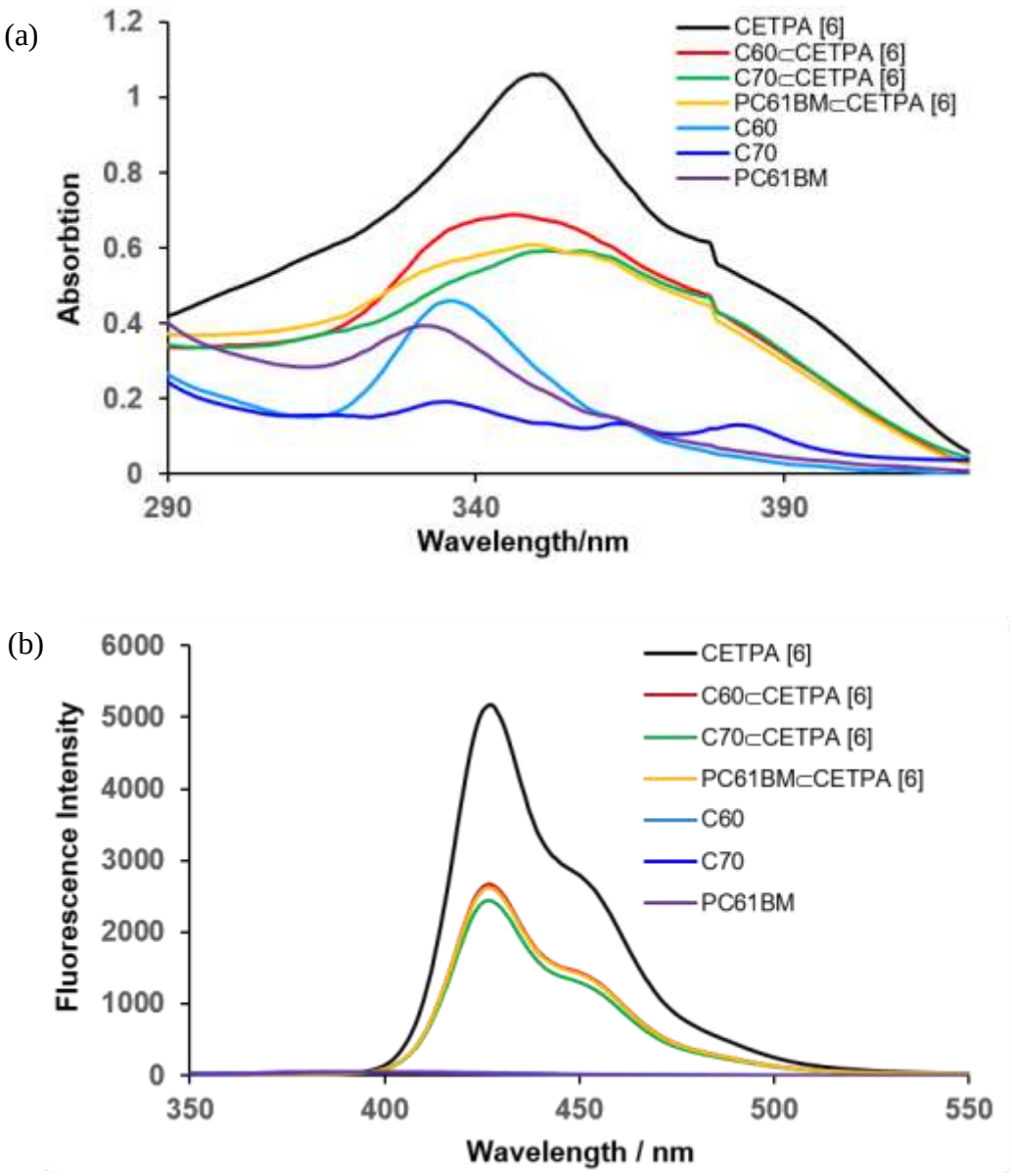

Fig. S21 (a) UV-vis and (b) fluorescence (λ_{ex} = 300 nm in toluene, 5×10^{-6} M, 298 K) spectra of **CETPA [6]**, C_{60}⊂ **CETPA [6]**, C_{70}⊂ **CETPA [6]**, $PC_{61}BM$⊂ **CETPA [6]**, C_{60}, C_{70} and $PC_{61}BM$.

4. Determination of binding stoichiometries

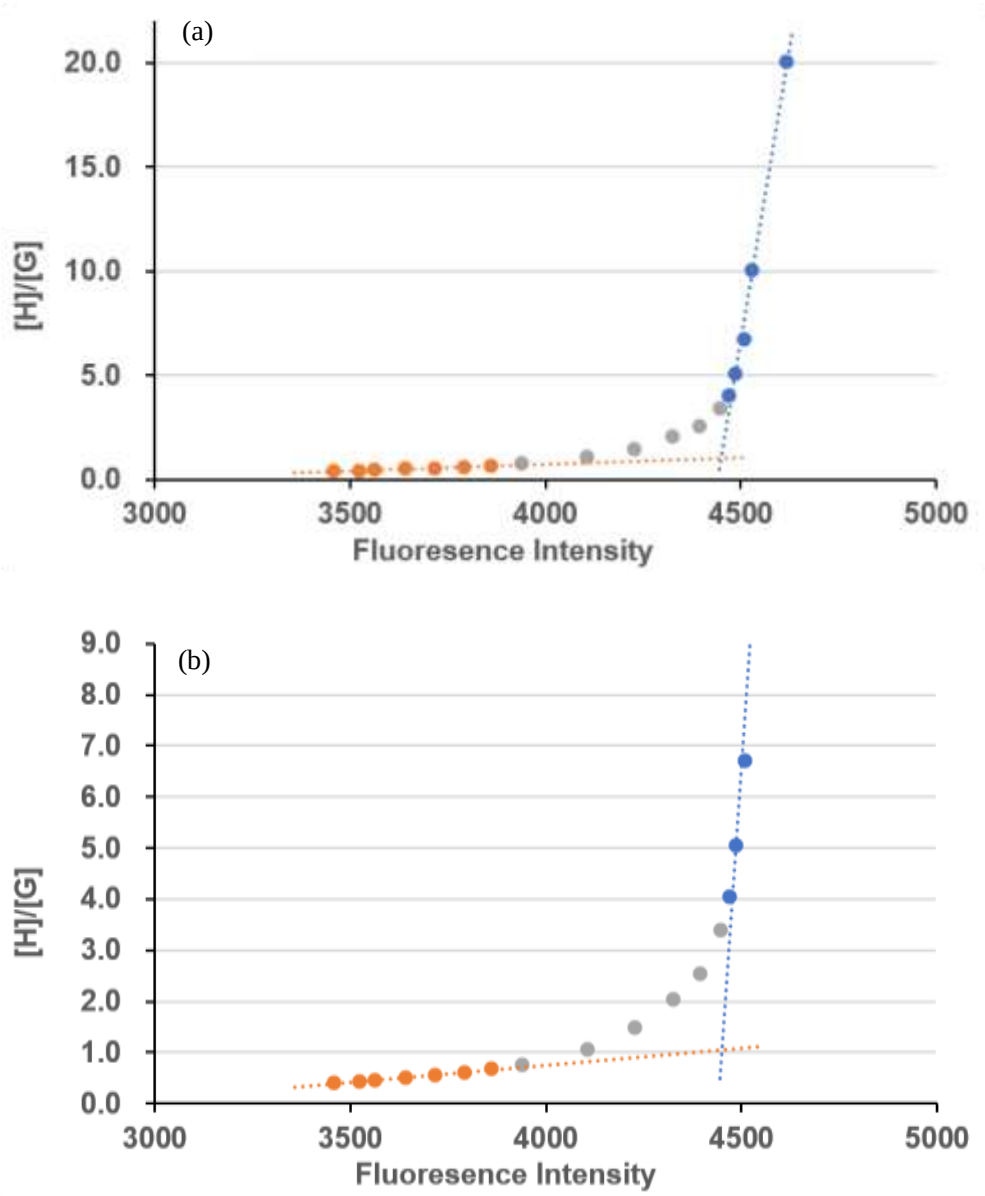

Fig. S22 (a) Mole ratio plot for the complexation between **COTPA [5]** and C_{60}, indicating a 1:1 stoichiometry; and (b) the enlarged plot of (a).

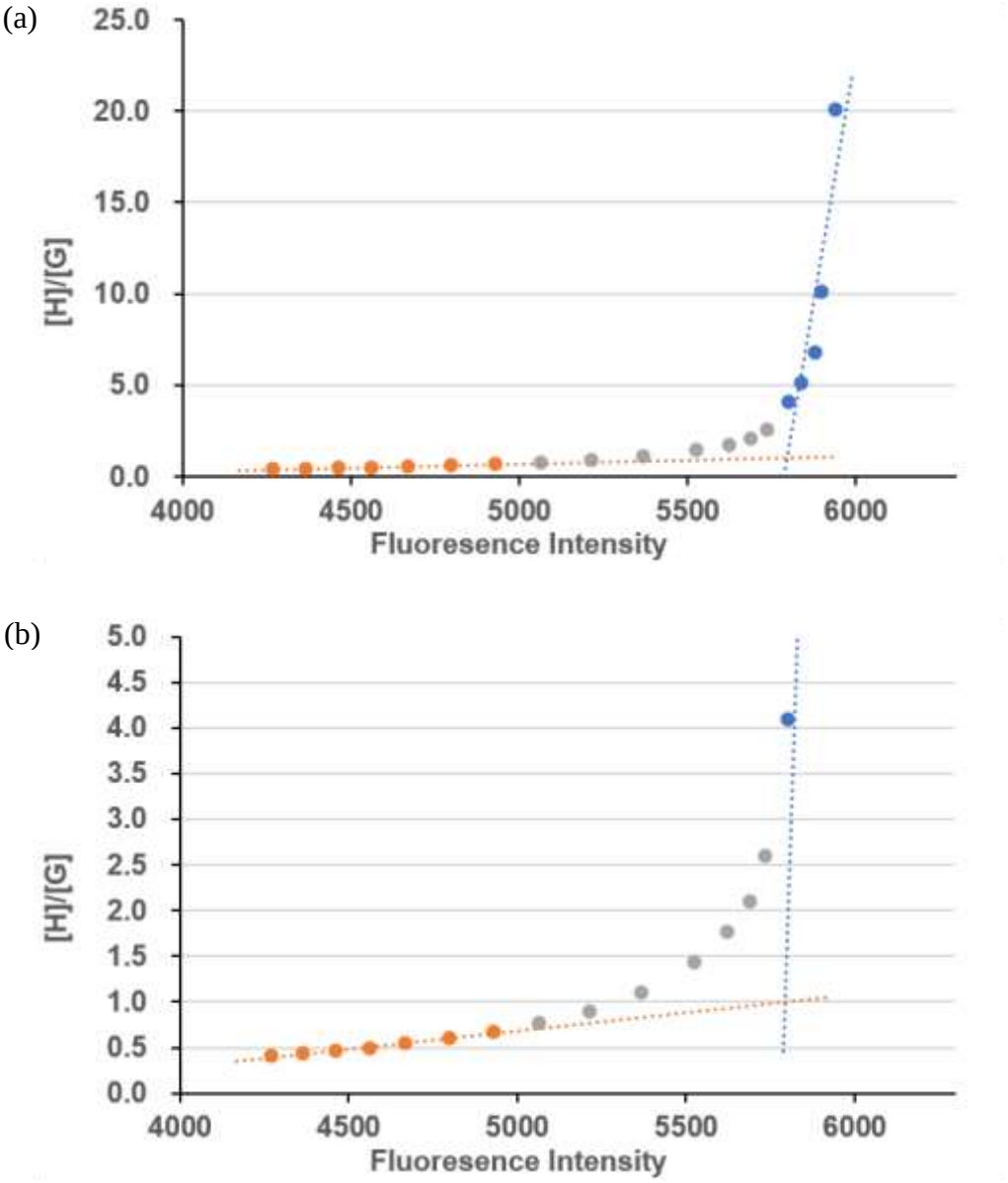

Fig. S23 (a) Mole ratio plot for the complexation between **COTPA [6]** and C_{60}, indicating a 1:1 stoichiometry, and (b) the enlarged plot of (a).

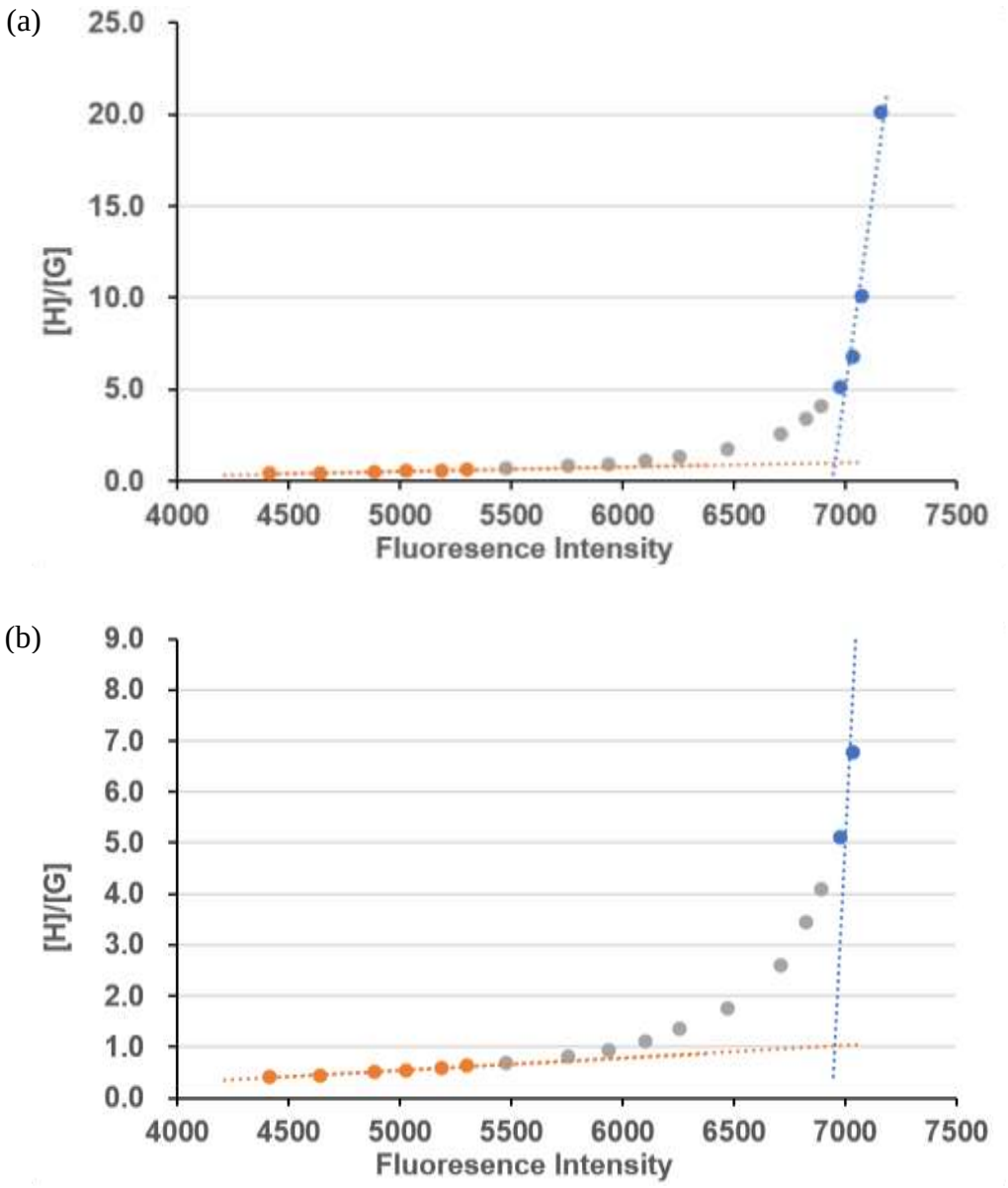

Fig. S24 (a) Mole ratio plot for the complexation between **COTPA [7]** and C_{60}, indicating a 1:1 stoichiometry, and (b) the enlarged plot of (a).

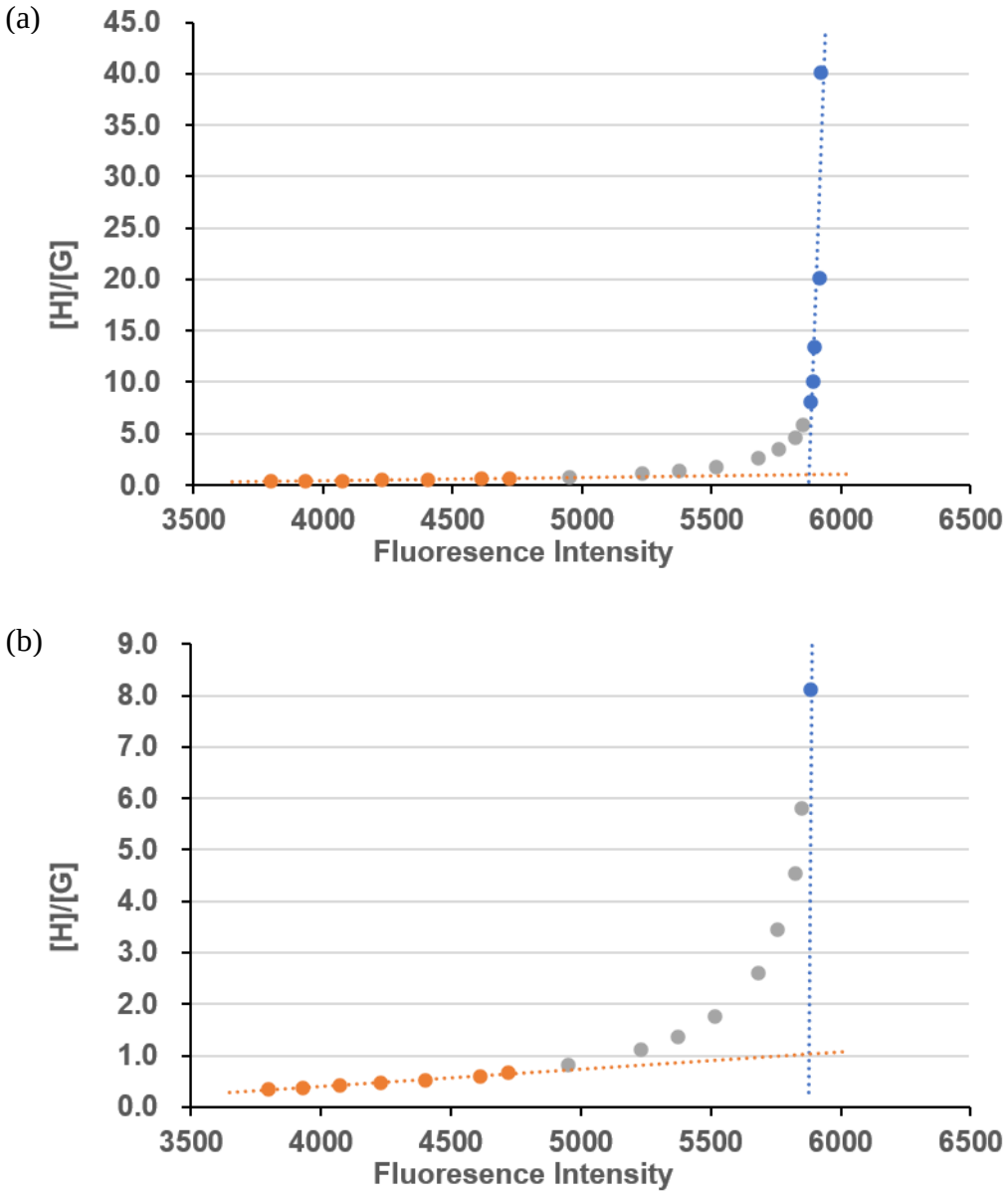

Fig. S25 (a) Mole ratio plot for the complexation between **CETPA [6]** and C_{60}, indicating a 1:1 stoichiometry, and (b) the enlarged plot of (a).

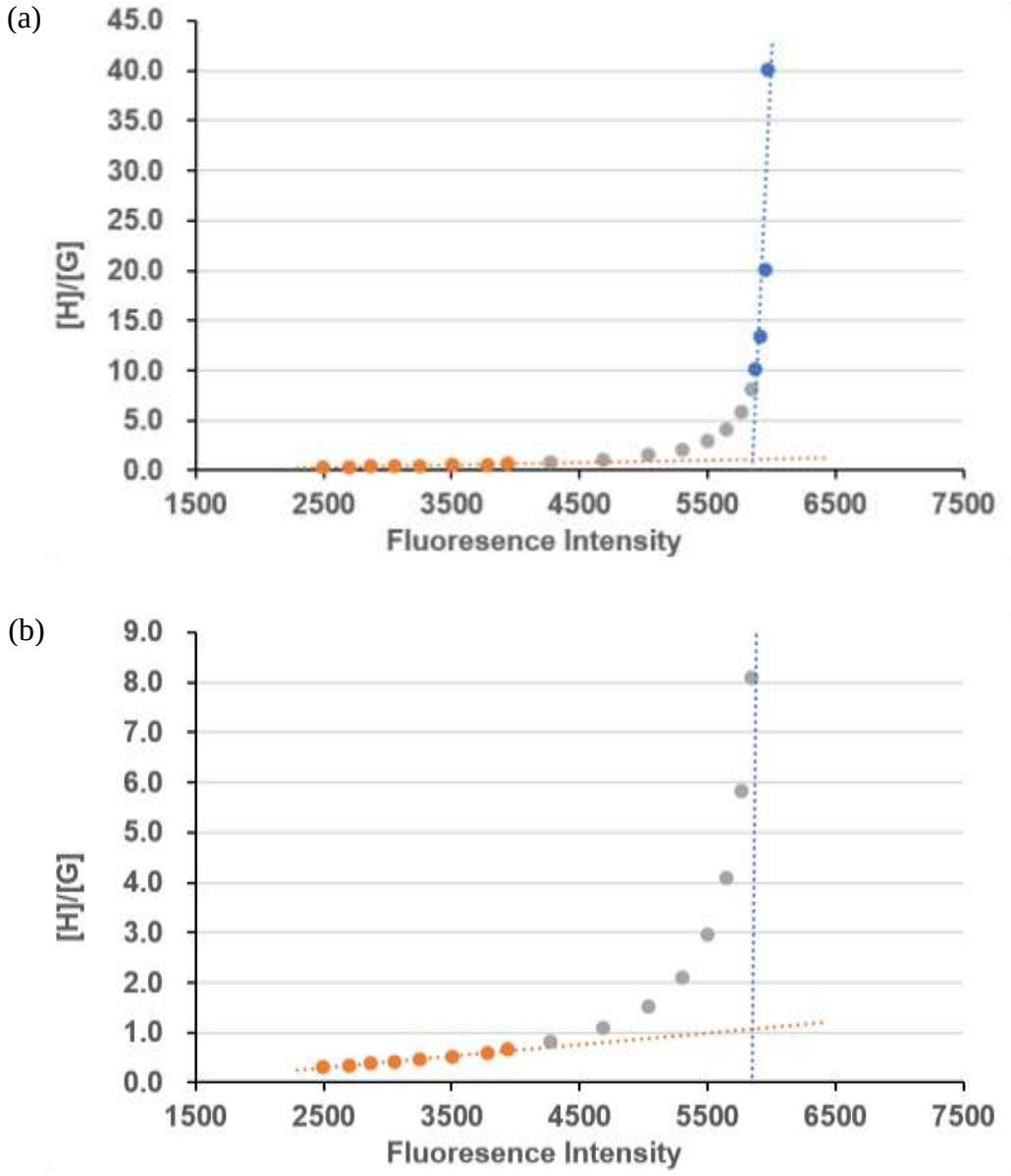

Fig. S26 (a) Mole ratio plot for the complexation between **COTPA [5]** and C_{70}, indicating a 1:1 stoichiometry, and (b) the enlarged plot of (a).

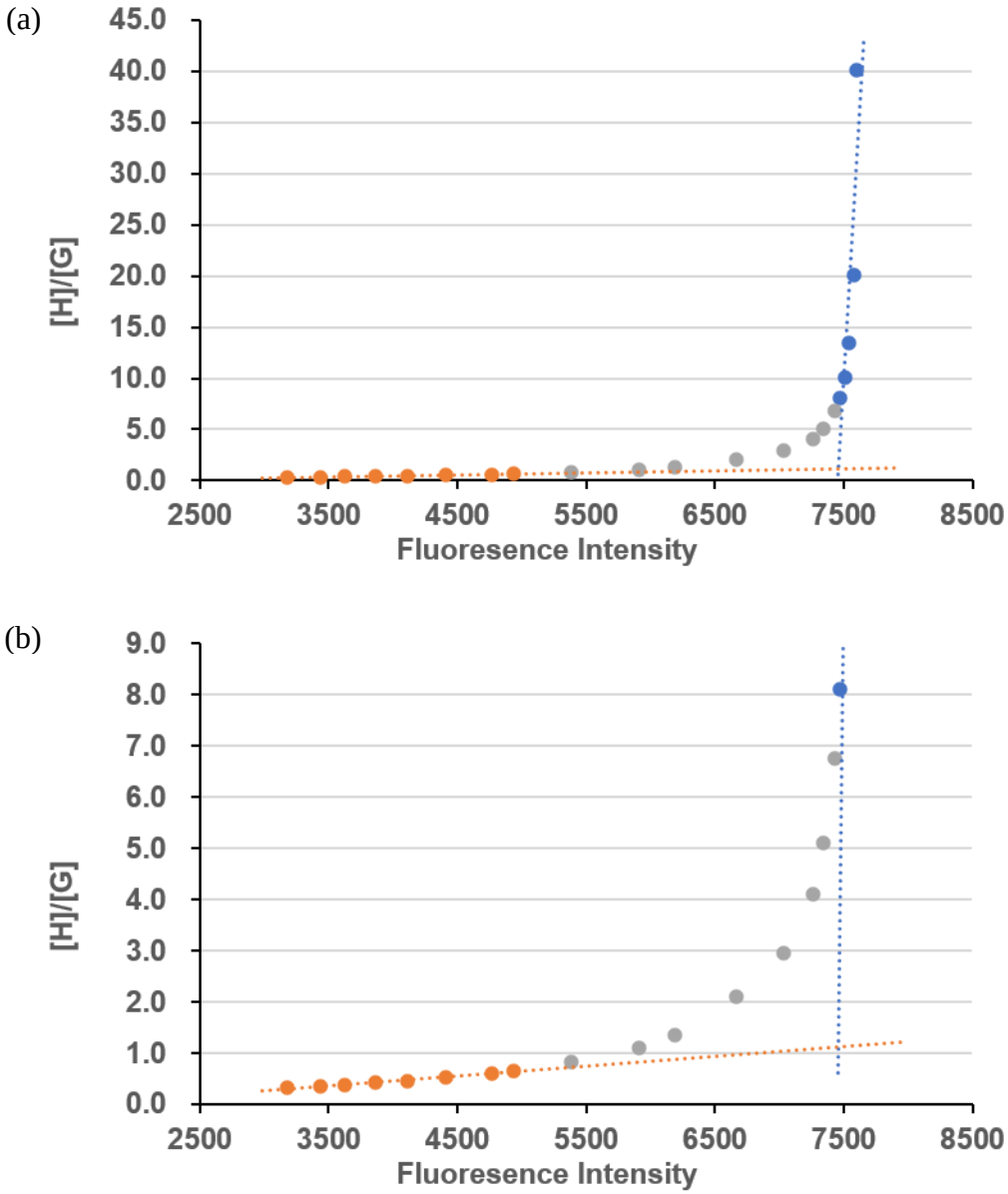

Fig. S27 (a) Mole ratio plot for the complexation between **COTPA [6]** and C_{70}, indicating a 1:1 stoichiometry, and (b) the enlarged plot of (a).

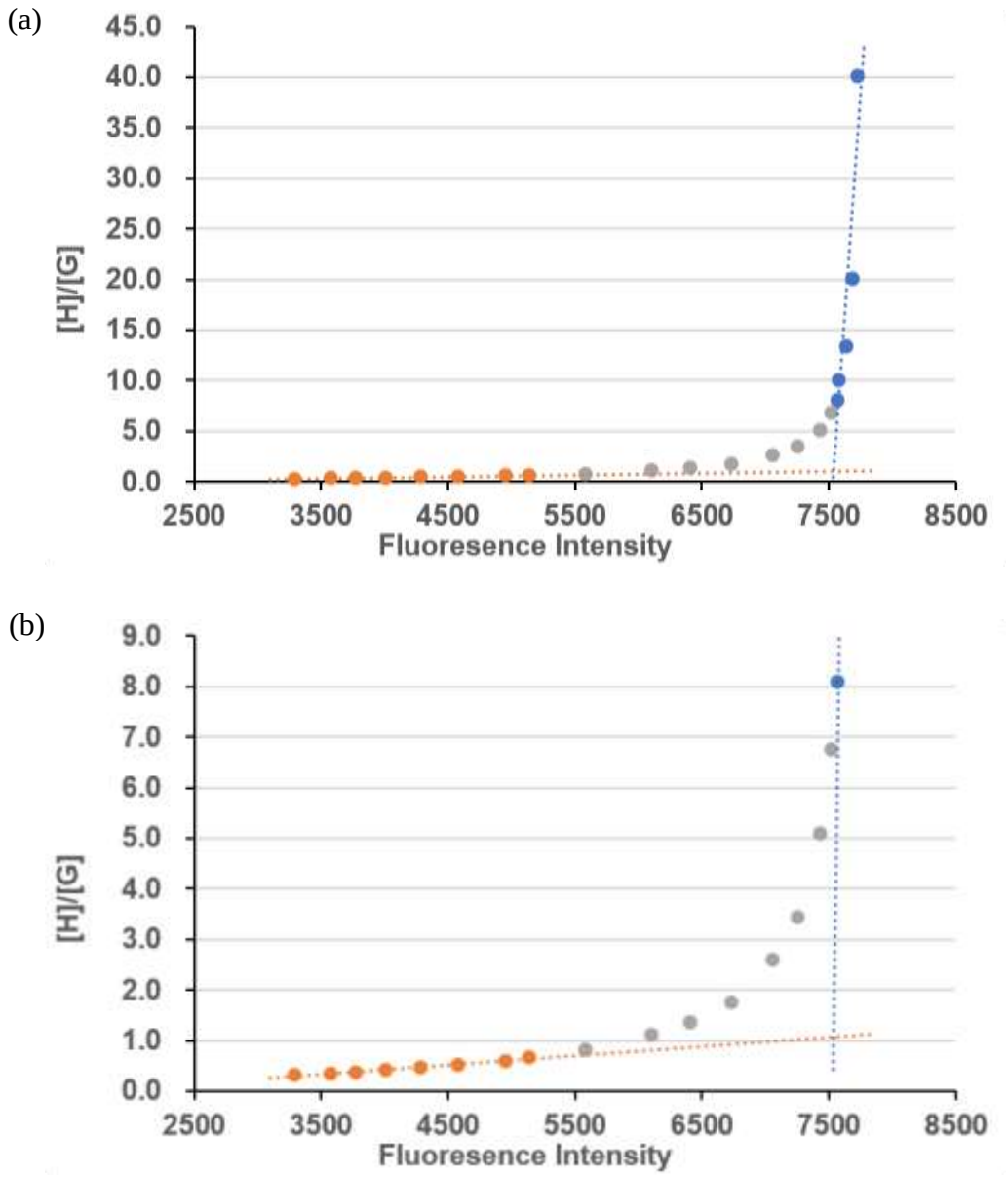

Fig. S28 (a) Mole ratio plot for the complexation between **COTPA [7]** and C_{70}, indicating a 1:1 stoichiometry, and (b) the enlarged plot of (a).

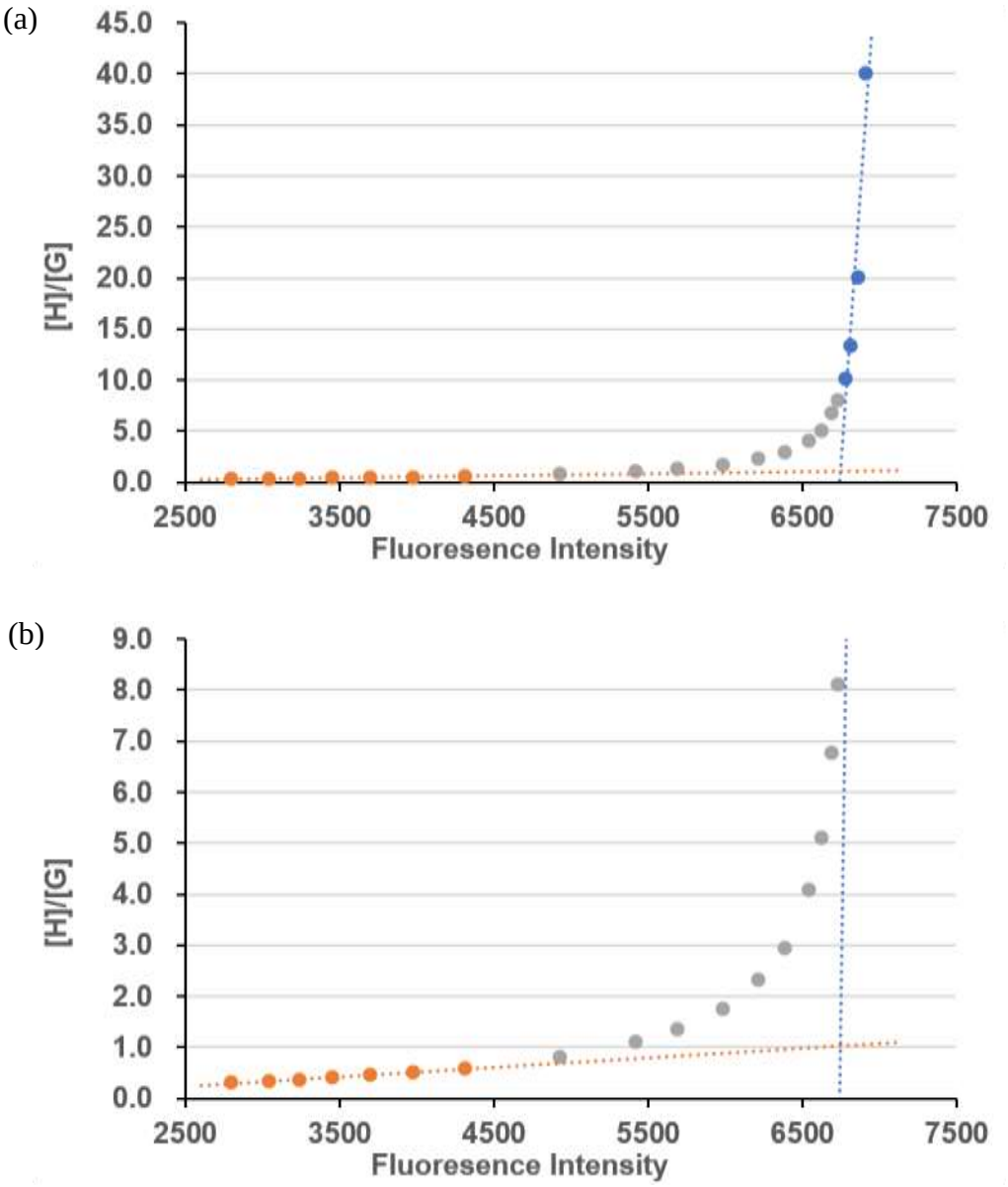

Fig. S29 (a) Mole ratio plot for the complexation between **CETPA [6]** and C_{70}, indicating a 1:1 stoichiometry, and (b) the enlarged plot of (a).

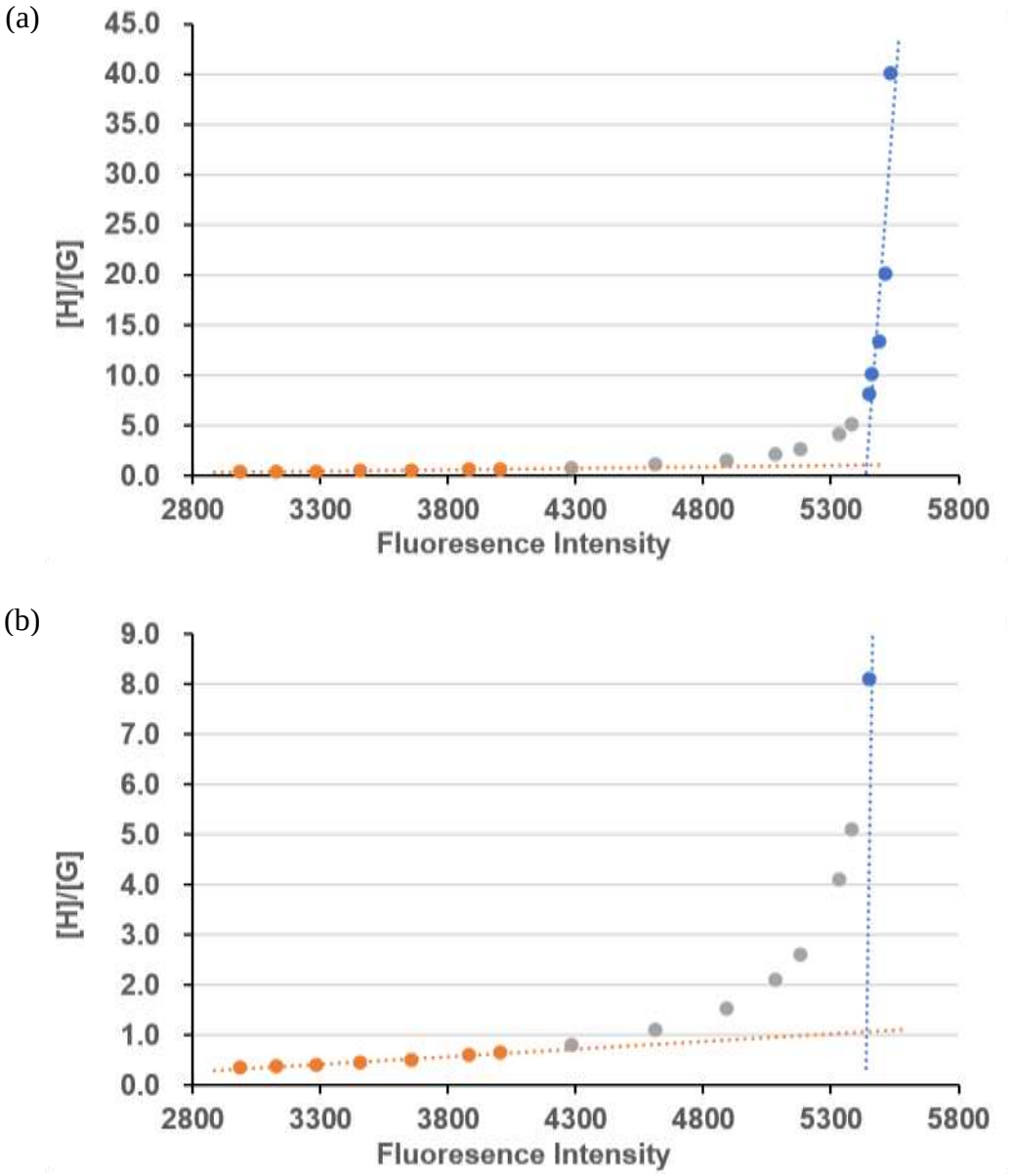

Fig. S30 (a) Mole ratio plot for the complexation between **COTPA [5]** and $PC_{61}BM$, indicating a 1:1 stoichiometry, and (b) the enlarged plot of (a).

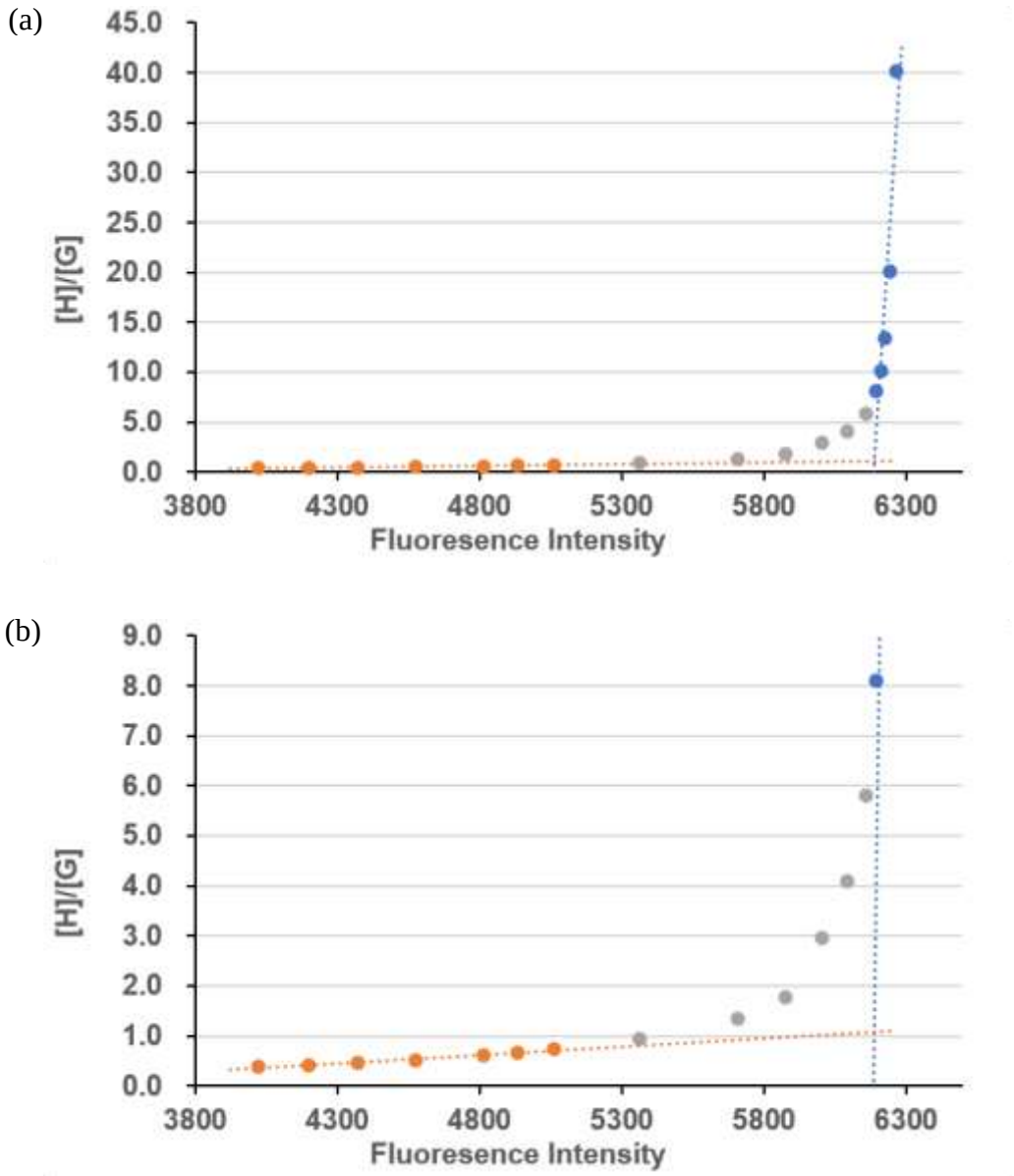

Fig. S31 (a) Mole ratio plot for the complexation between **COTPA [6]** and $PC_{61}BM$, indicating a 1:1 stoichiometry, and (b) the enlarged plot of (a).

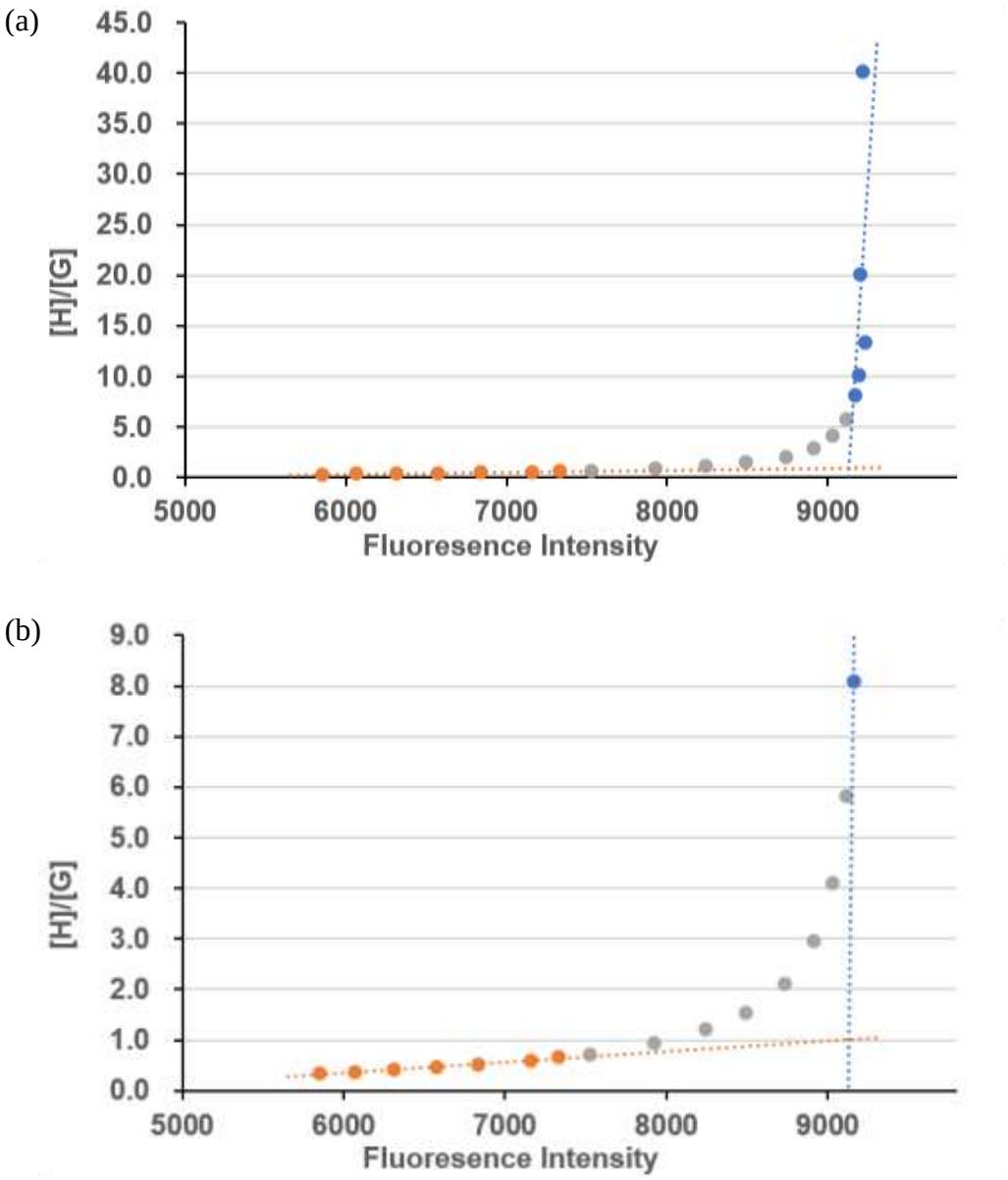

Fig. S32 (a) Mole ratio plot for the complexation between **COTPA [7]** and $PC_{61}BM$, indicating a 1:1 stoichiometry, and (b) the enlarged plot of (a).

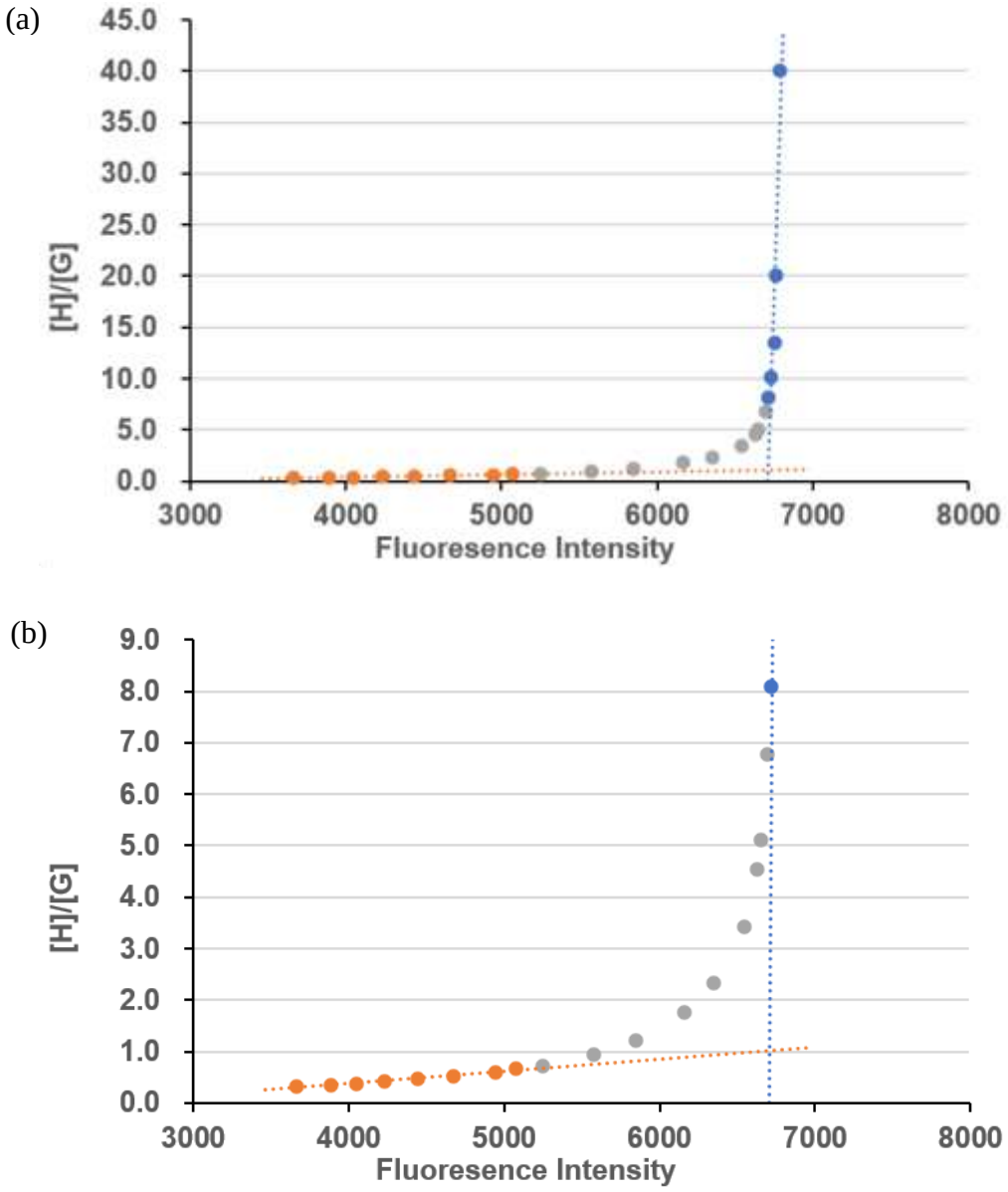

Fig. S33 (a) Mole ratio plot for the complexation between **CETPA [6]** and $PC_{61}BM$, indicating a 1:1 stoichiometry, and (b) the enlarged plot of (a).

5. Measurement of binding constants (K_a)

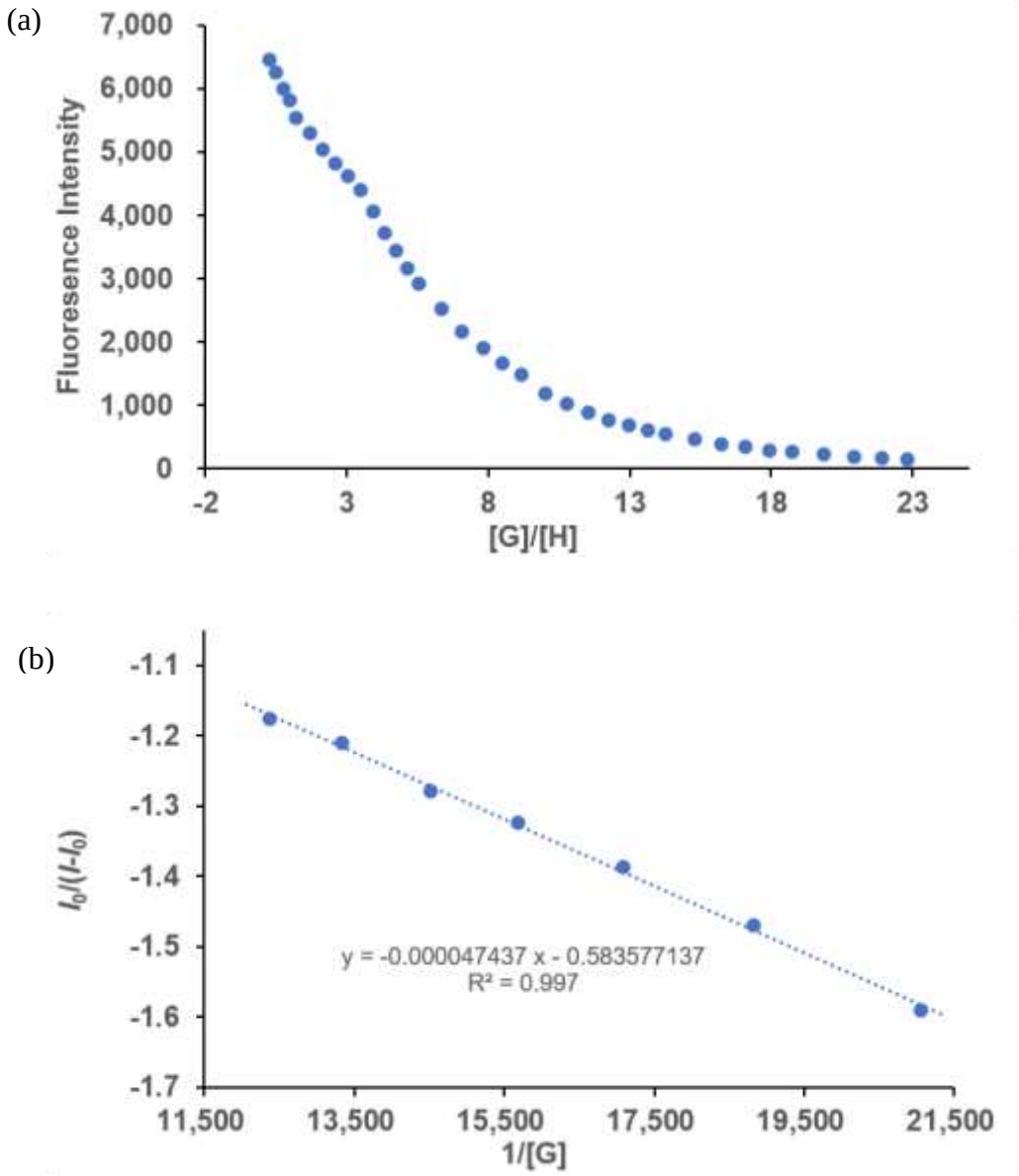

Fig. S34 (a) The fluorescence intensity of **COTPA [5]** (5×10^{-6} M, λ_{ex} = 300 nm) upon addition of C_{60} in toluene at 298 K; and (b) relationship between $I_0/(I - I_0)$ and $1/[G]_0$ for the complexation between **COTPA [5]** and C_{60} in toluene at 298 K, wherein I and I_0 are the emission intensity at 423 nm in 298 K with concentration of $[G]_0$ and 0, respectively.

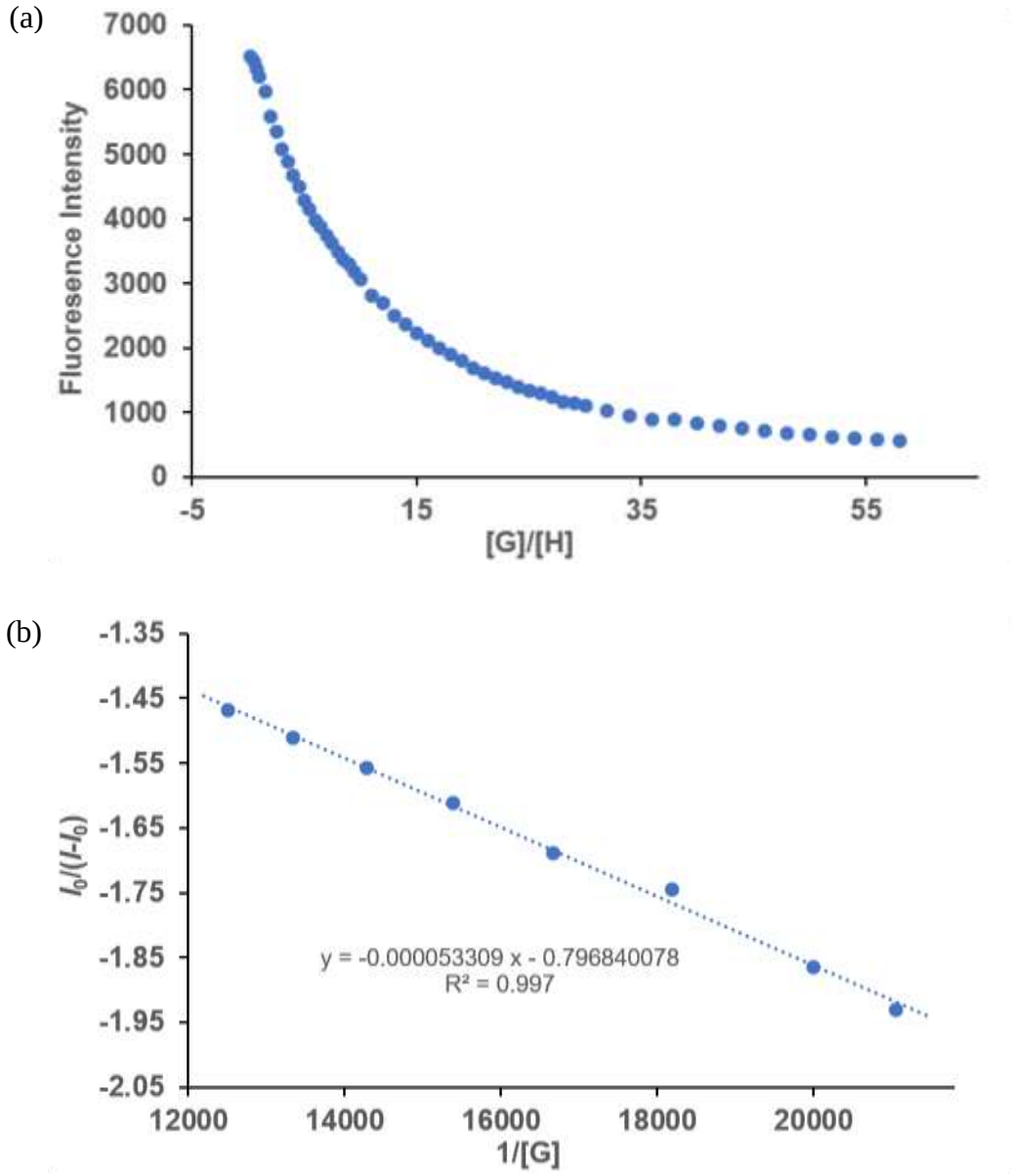

Fig. S35 (a) The fluorescence intensity of **COTPA [6]** (5×10^{-6} M, λ_{ex} = 300 nm) upon addition of C_{60} in toluene at 298 K; and (b) relationship between $I_0/(I - I_0)$ and $1/[G]_0$ for the complexation between **COTPA [6]** and C_{60} in toluene at 298 K, wherein I and I_0 are the emission intensity at 421 nm in 298 K with concentration of $[G]_0$ and 0, respectively.

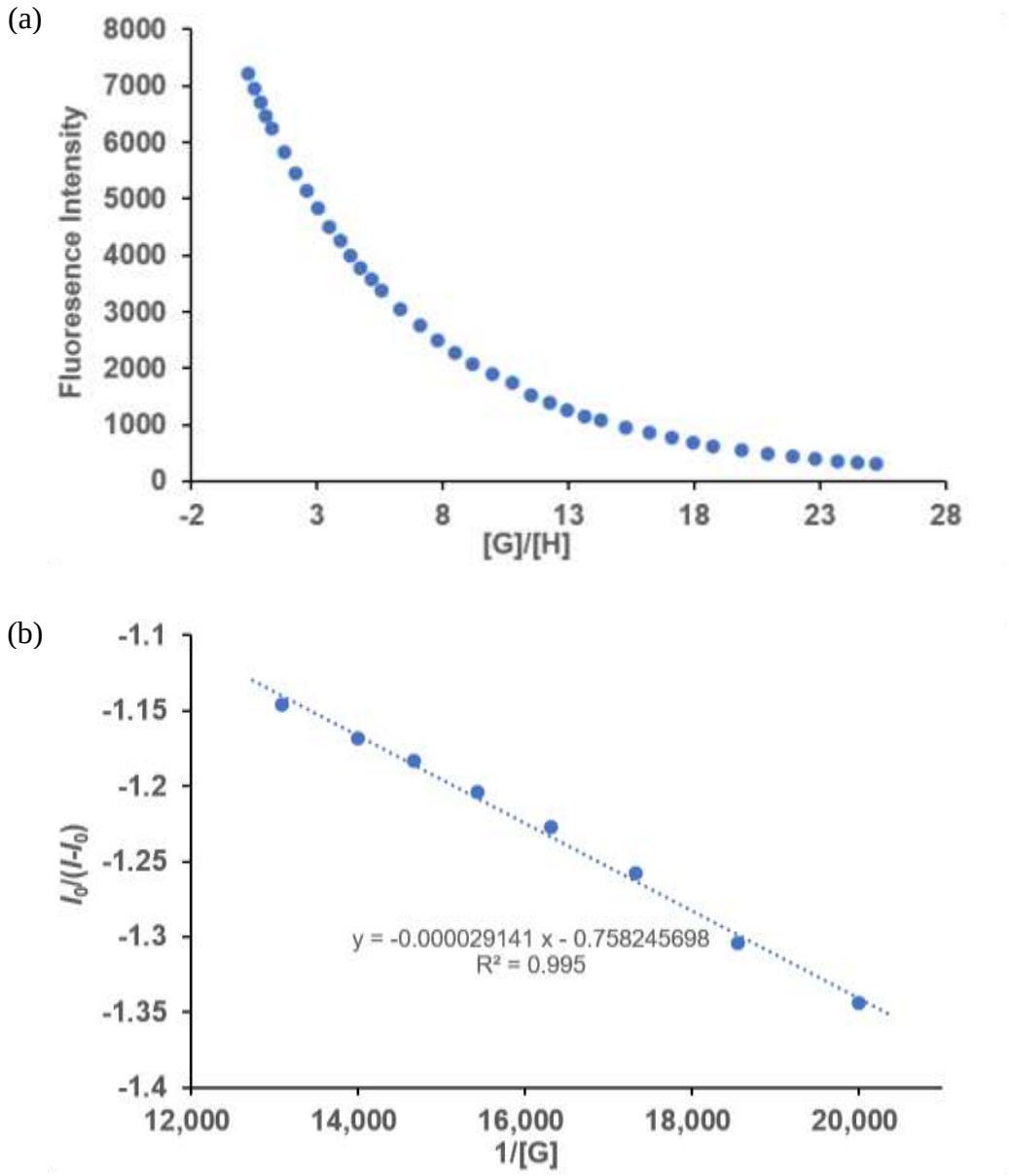

Fig. S36 (a) The fluorescence intensity of **COTPA [7]** (5×10^{-6} M, λ_{ex} = 300 nm) upon addition of C_{60} in toluene at 298 K; and (b) relationship between $I_0/(I - I_0)$ and $1/[G]_0$ for the complexation between **COTPA [7]** and C_{60} in toluene at 298 K, wherein I and I_0 are the emission intensity at 420 nm in 298 K with concentration of $[G]_0$ and 0, respectively.

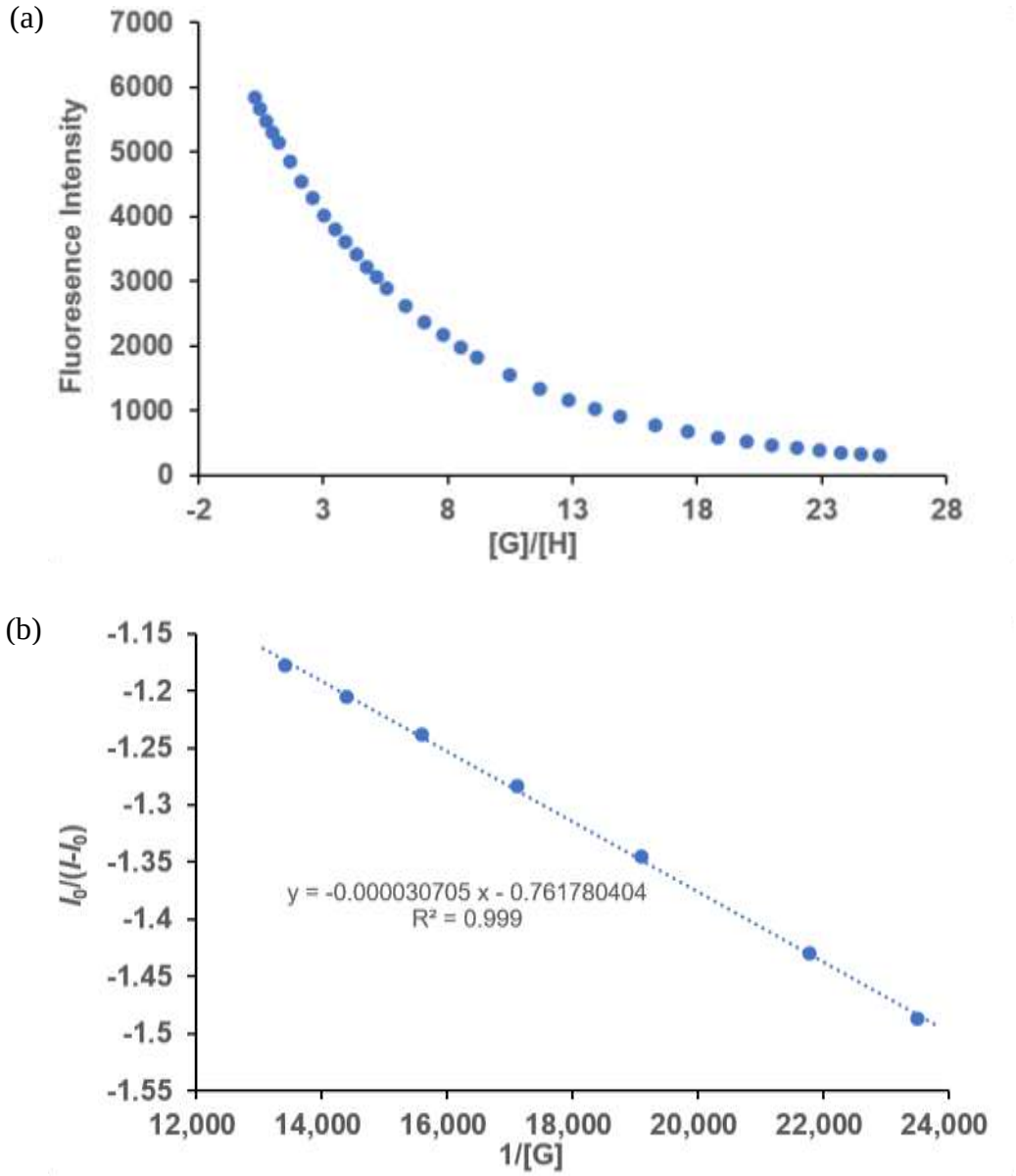

Fig. S37 (a) The fluorescence intensity of **CETPA [6]** (5×10^{-6} M, λ_{ex} = 300 nm) upon addition of C_{60} in toluene at 298 K; and (b) relationship between $I_0/(I - I_0)$ and $1/[G]_0$ for the complexation between **CETPA [6]** and C_{60} in toluene at 298 K, wherein I and I_0 are the emission intensity at 427 nm in 298 K with concentration of $[G]_0$ and 0, respectively.

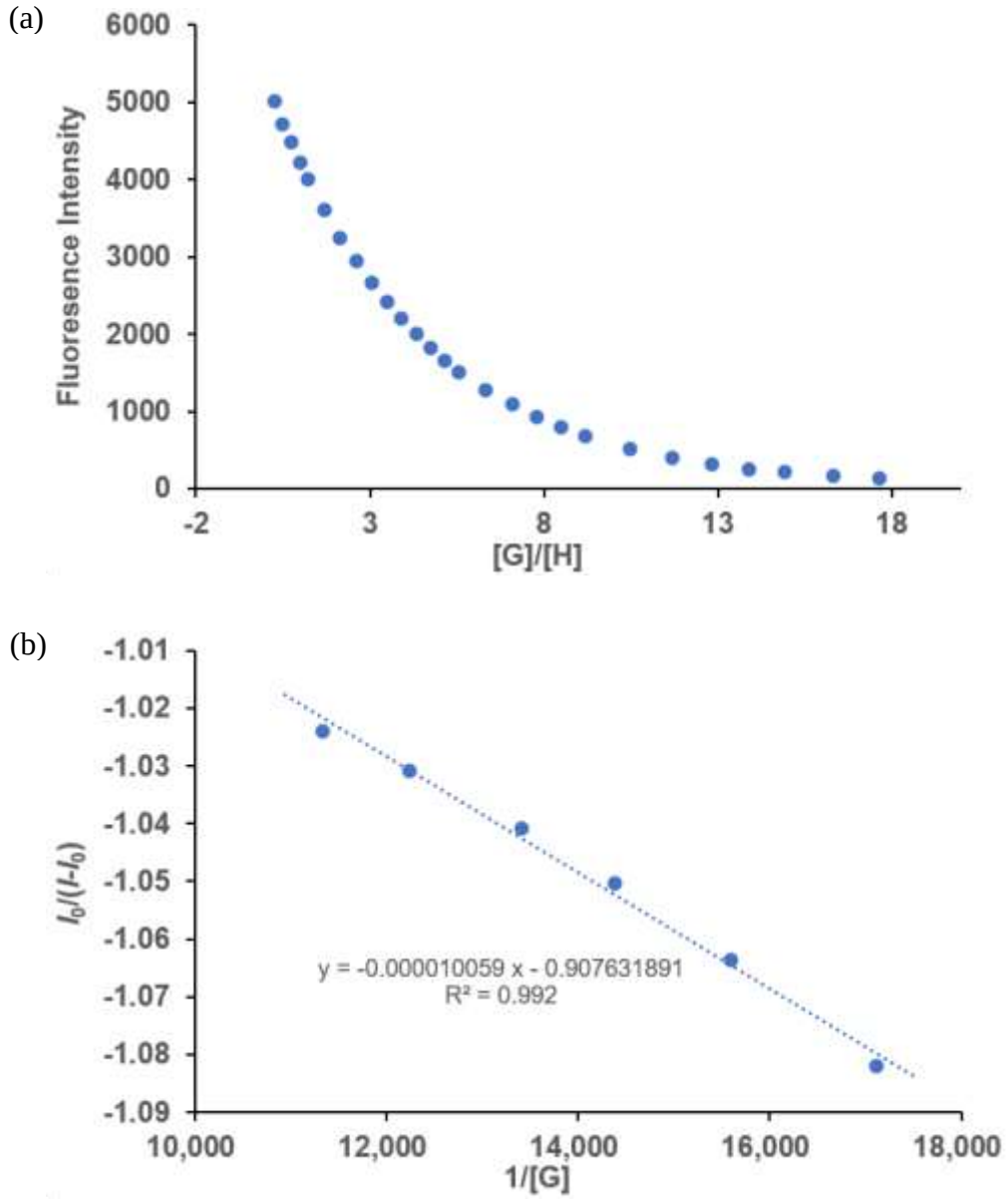

Fig. S38 (a) The fluorescence intensity of **COTPA [5]** (5×10^{-6} M, λ_{ex} = 300 nm) upon addition of $PC_{61}BM$ in toluene at 298 K; and (b) relationship between $I_0/(I - I_0)$ and $1/[G]_0$ for the complexation between **COTPA [5]** and $PC_{61}BM$ in toluene at 298 K, wherein I and I_0 are the emission intensity at 423 nm in 298 K with concentration of $[G]_0$ and 0, respectively.

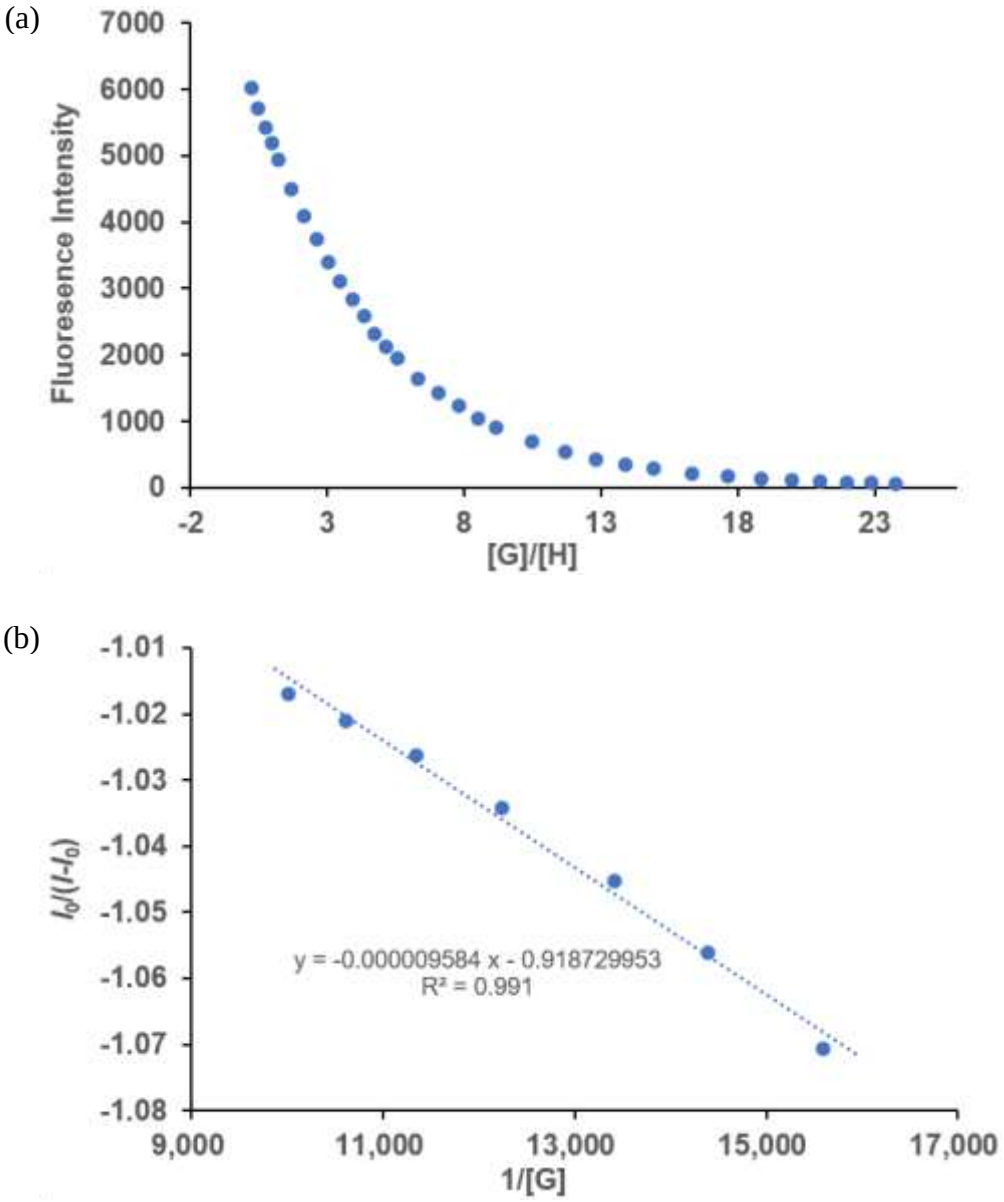

Fig. S39 (a) The fluorescence intensity of **COTPA [6]** (5×10^{-6} M, λ_{ex} = 300 nm) upon addition of $PC_{61}BM$ in toluene at 298 K; and (b) relationship between $I_0/(I - I_0)$ and $1/[G]_0$ for the complexation between **COTPA [6]** and $PC_{61}BM$ in toluene at 298 K, wherein I and I_0 are the emission intensity at 421 nm in 298 K with concentration of $[G]_0$ and 0, respectively.

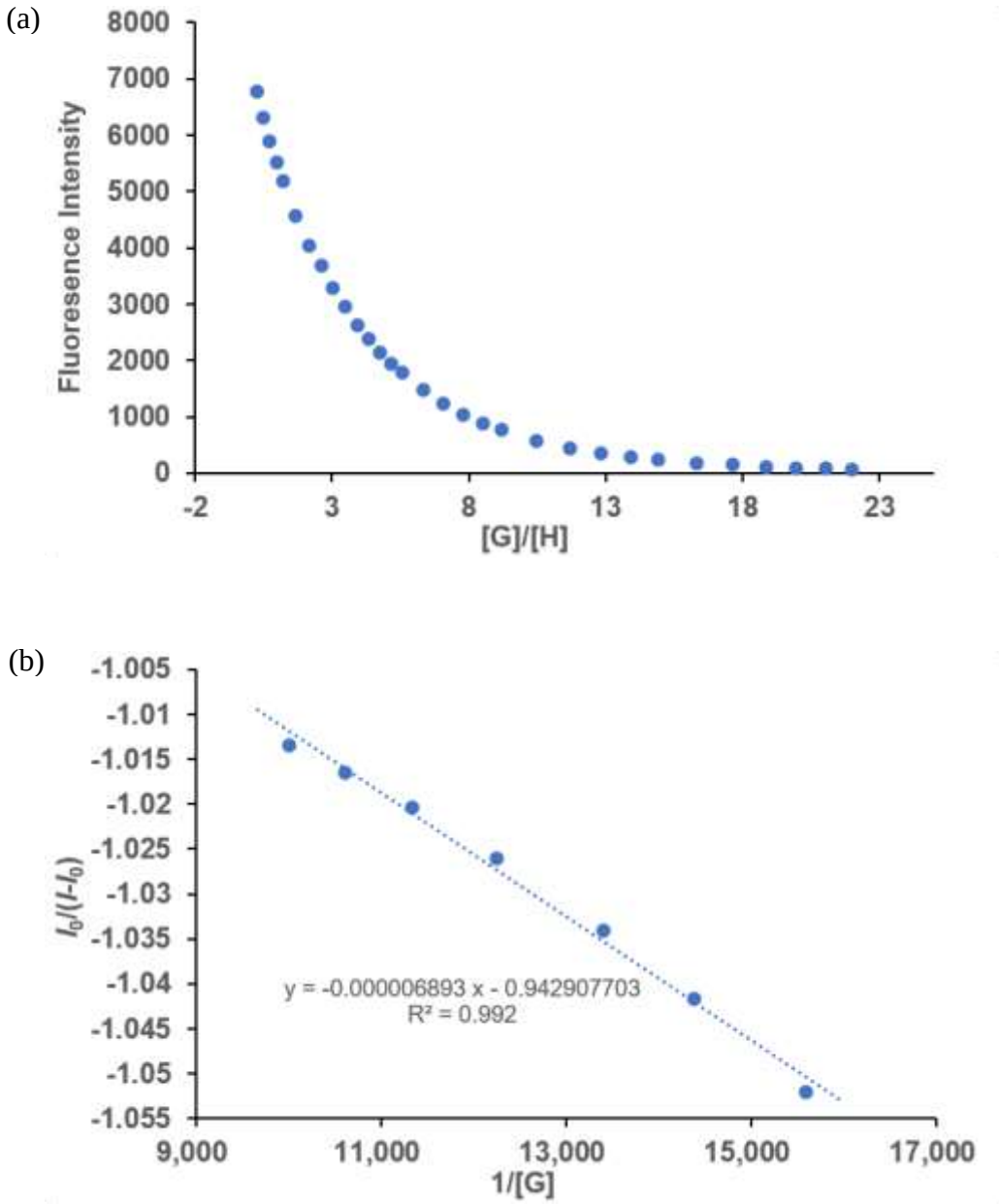

Fig. S40 (a) The fluorescence intensity of **COTPA [7]** (5×10^{-6} M, λ_{ex} = 300 nm) upon addition of $PC_{61}BM$ in toluene at 298 K; and (b) relationship between $I_0/(I - I_0)$ and $1/[G]_0$ for the complexation between **COTPA [7]** and $PC_{61}BM$ in toluene at 298 K, wherein I and I_0 are the emission intensity at 420 nm in 298 K with concentration of $[G]_0$ and 0, respectively.

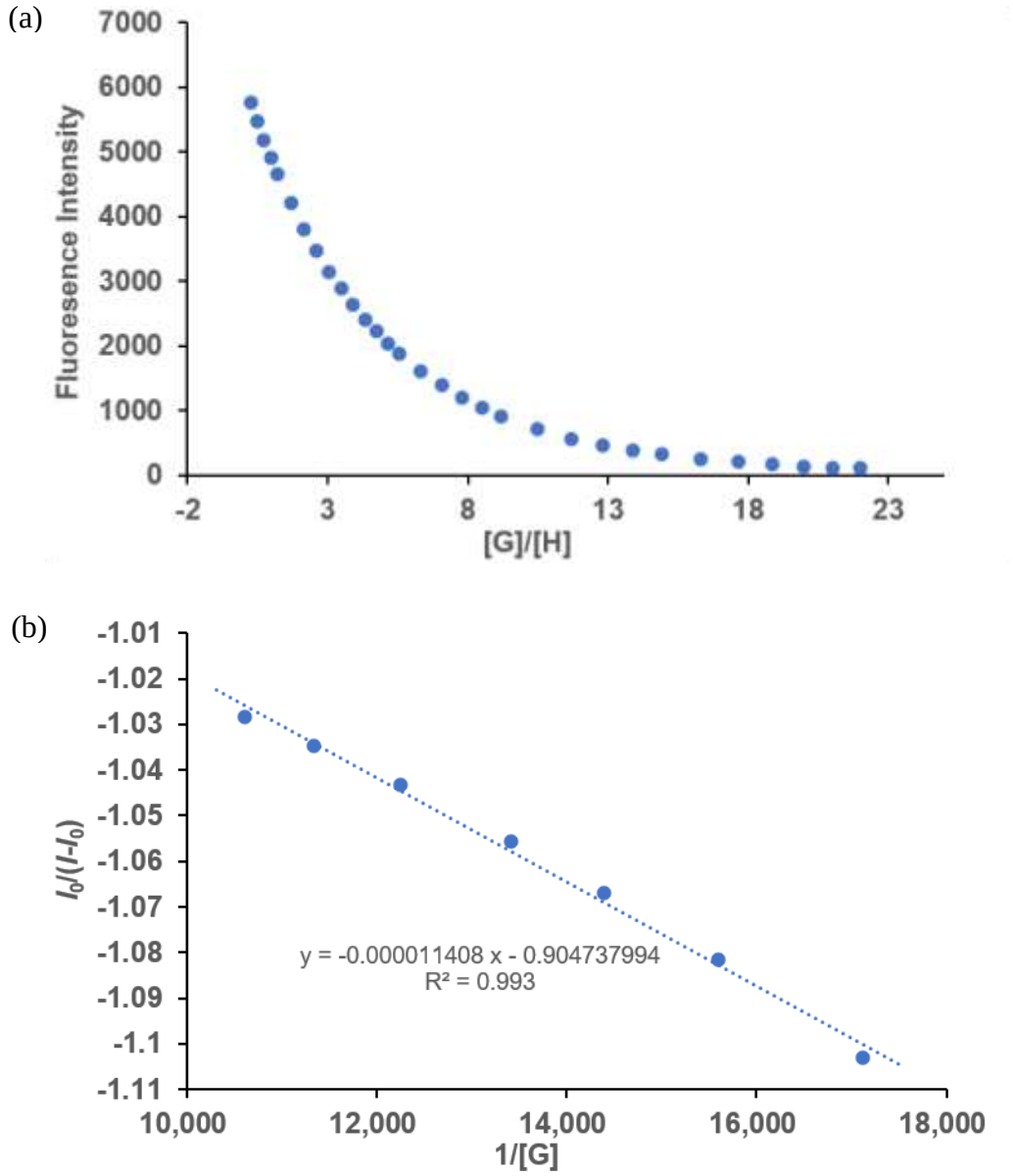

Fig. S41 (a) The fluorescence intensity of **CETPA [6]** (5×10^{-6} M, λ_{ex} = 300 nm) upon addition of $PC_{61}BM$ in toluene at 298 K; and (b) relationship between $I_0/(I - I_0)$ and $1/[G]_0$ for the complexation between **CETPA [6]** and $PC_{61}BM$ in toluene at 298 K, wherein I and I_0 are the emission intensity at 427 nm in 298 K with concentration of $[G]_0$ and 0, respectively.

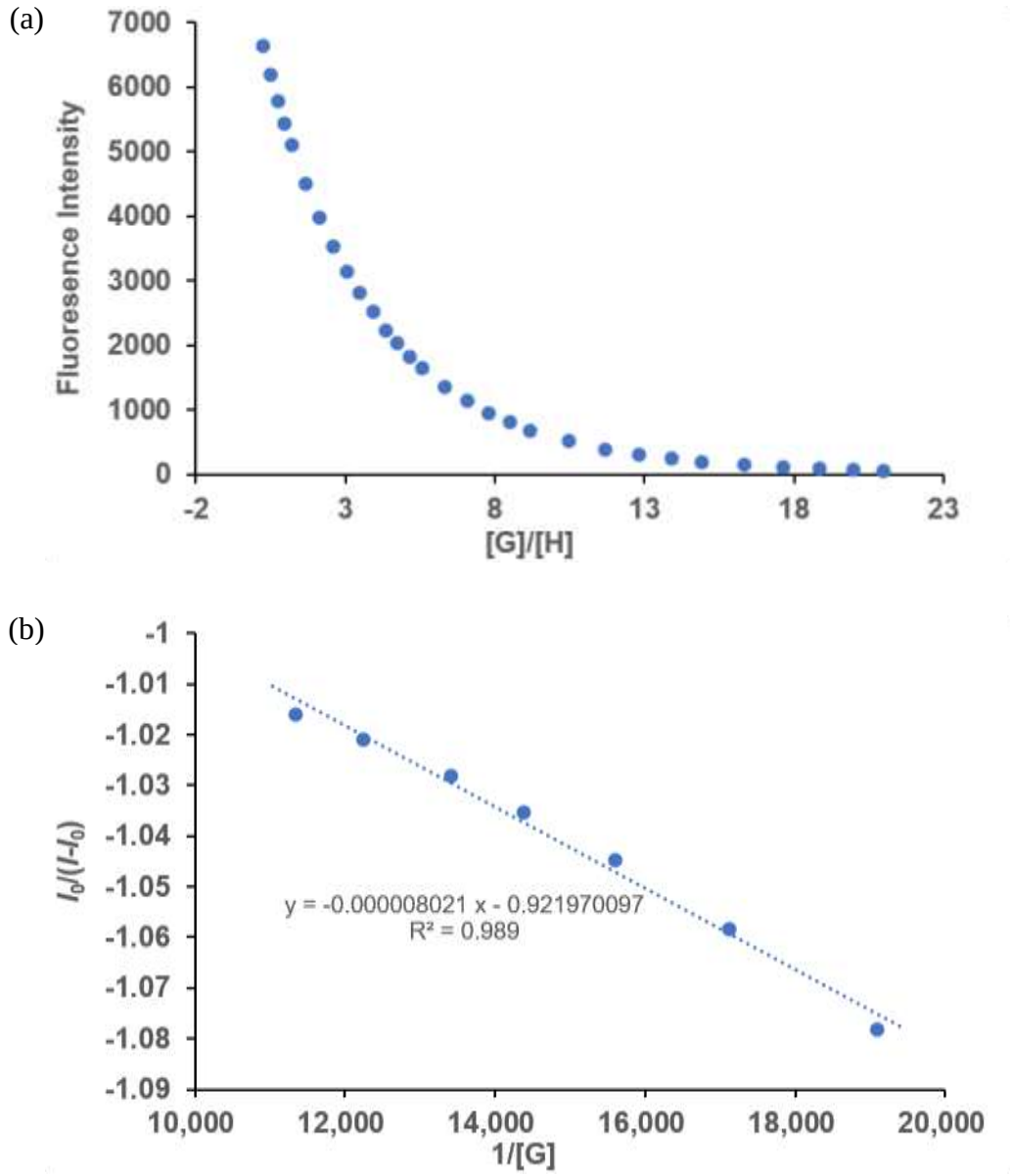

Fig. S42 (a) The fluorescence intensity of **COTPA [5]** (5×10^{-6} M, λ_{ex} = 300 nm) upon addition of C_{70} in toluene at 298 K; and (b) relationship between $I_0/(I - I_0)$ and $1/[G]_0$ for the complexation between **COTPA [5]** and C_{70} in toluene at 298 K, wherein I and I_0 are the emission intensity at 423 nm in 298 K with concentration of $[G]_0$ and 0, respectively.

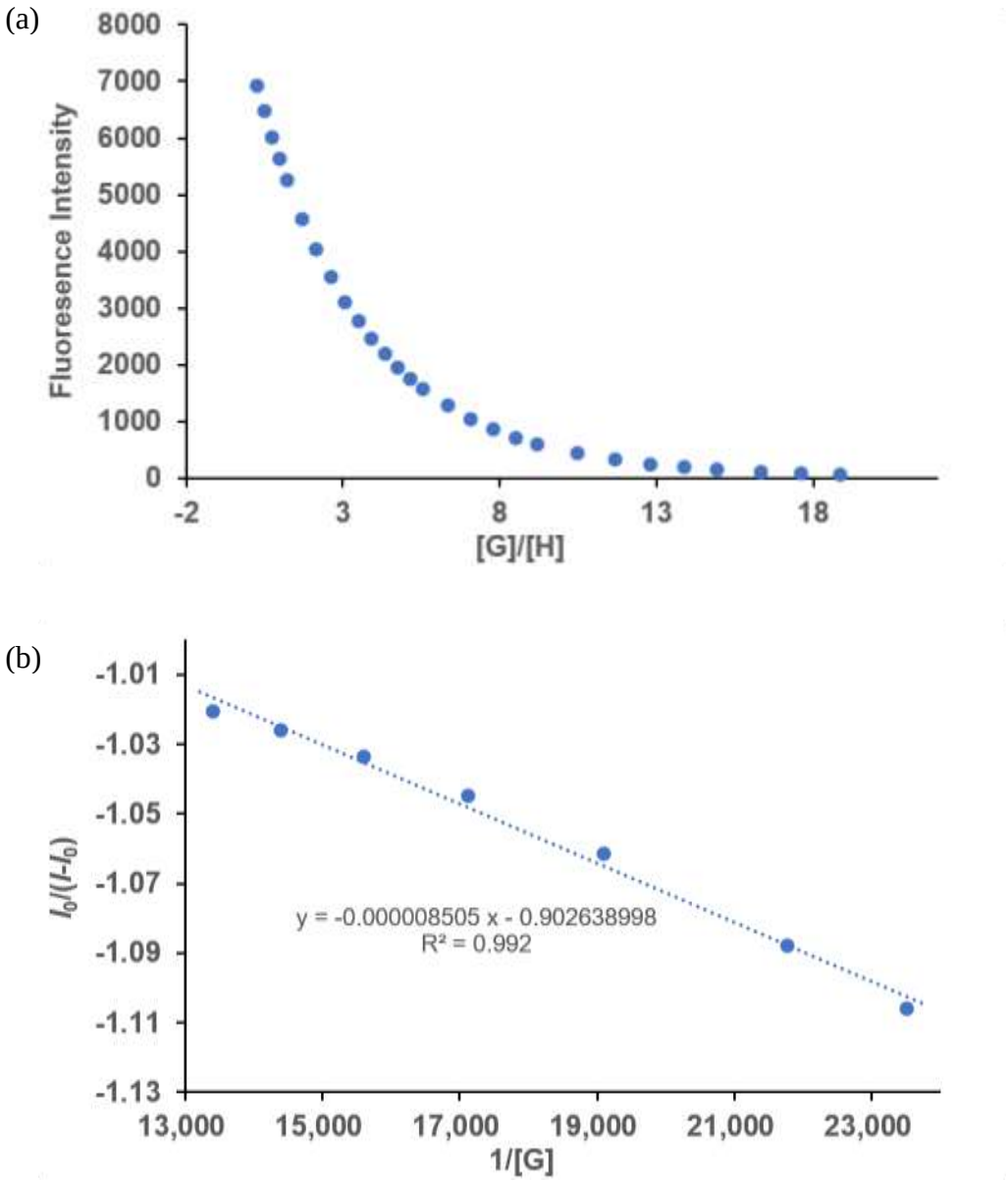

Fig. S43 (a) The fluorescence intensity of **COTPA [6]** (5×10^{-6} M, λ_{ex} = 300 nm) upon addition of C_{70} in toluene at 298 K; and (b) relationship between $I_0/(I - I_0)$ and $1/[G]_0$ for the complexation between **COTPA [6]** and C_{70} in toluene at 298 K, wherein I and I_0 are the emission intensity at 421 nm in 298 K with concentration of $[G]_0$ and 0, respectively.

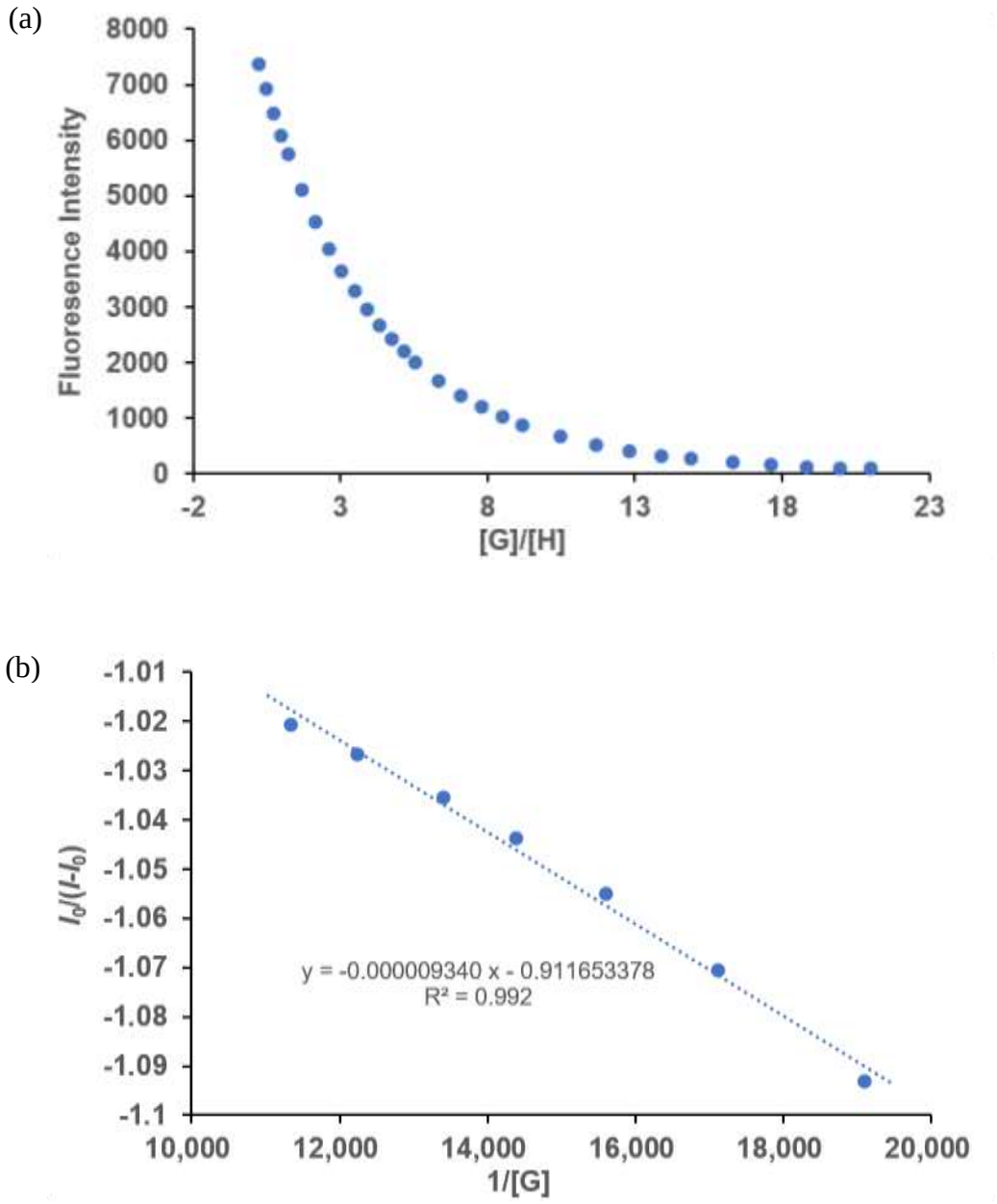

Fig. S44 (a) The fluorescence intensity of **COTPA [7]** (5×10^{-6} M, λ_{ex} = 300 nm) upon addition of C_{70} in toluene at 298 K; and (b) relationship between $I_0/(I - I_0)$ and $1/[G]_0$ for the complexation between **COTPA [7]** and C_{70} in toluene at 298 K, wherein I and I_0 are the emission intensity at 420 nm in 298 K with concentration of $[G]_0$ and 0, respectively.

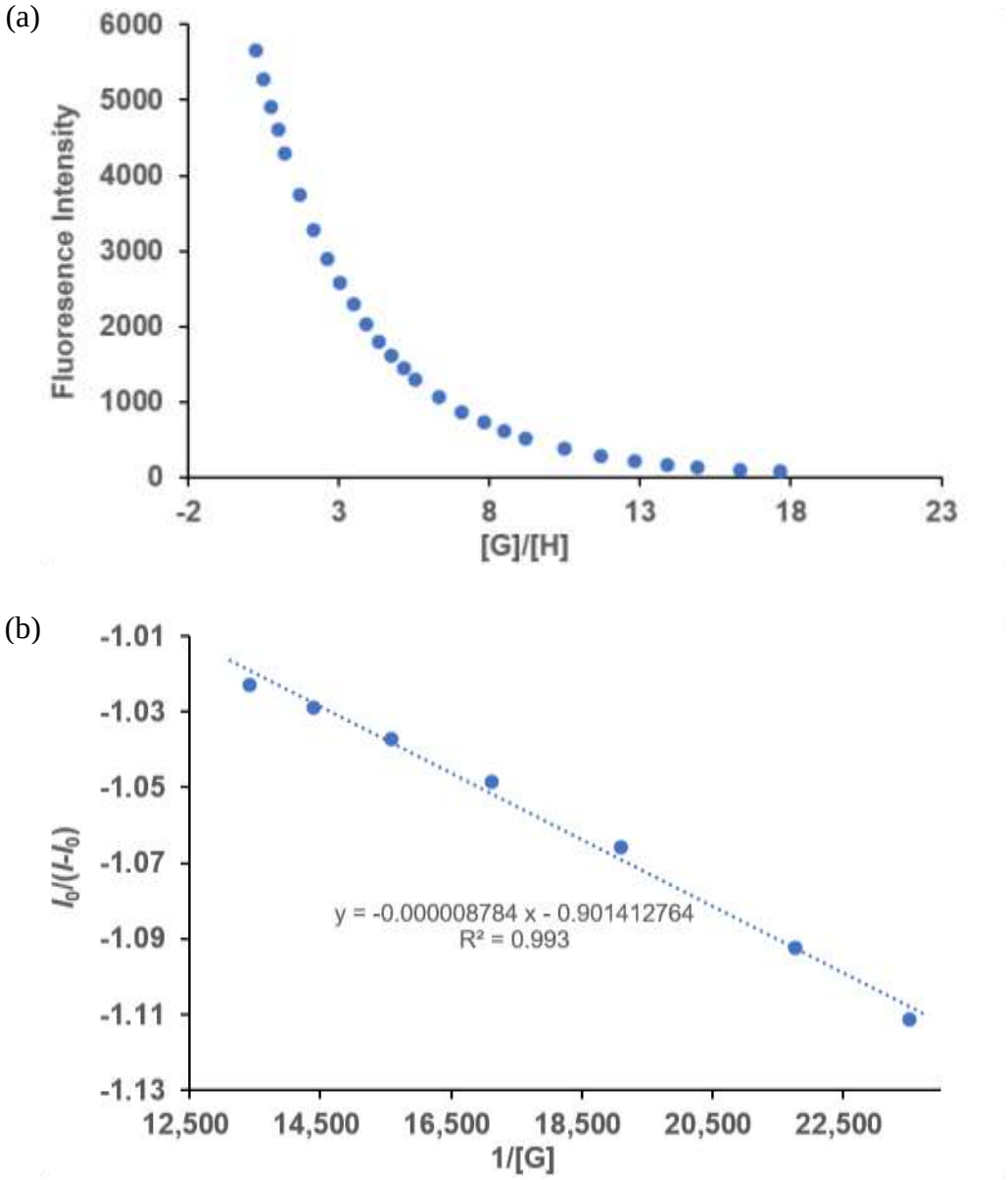

Fig. S45 (a) The fluorescence intensity of **CETPA [6]** (5×10^{-6} M, λ_{ex} = 300 nm) upon addition of C_{70} in toluene at 298 K; and (b) relationship between $I_0/(I - I_0)$ and $1/[G]_0$ for the complexation between **CETPA [6]** and C_{70} in toluene at 298 K, wherein I and I_0 are the emission intensity at 427 nm in 298 K with concentration of $[G]_0$ and 0, respectively.

6. Side view of DFT optimized structures

(a)

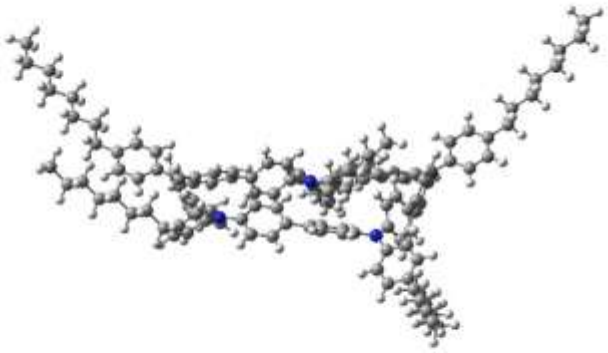

(b)

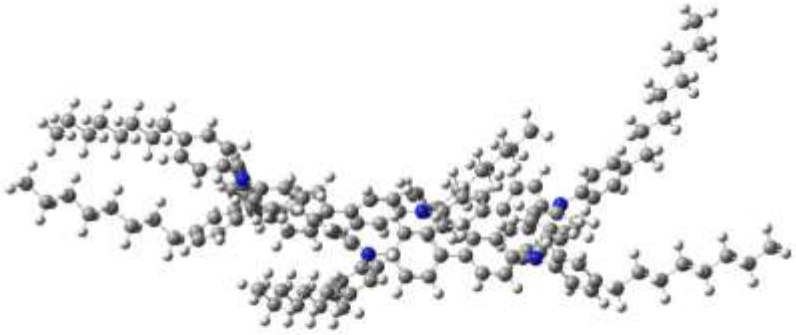

(c)

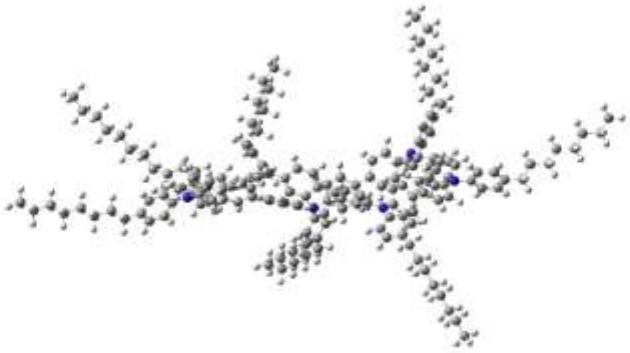

Fig. S46 The side view of DFT optimized structure of (a) **COTPA [5]**, (b) **COTPA [6]**, and (c) **COTPA [7]**.